

IMPERIAL

Final Report - Human & Biological Robotics (MSc) Project

Imperial College London, Department of Bioengineering

Developing a High-Performance Neural Logger for Closed-Loop Auditory Stimulation in Free- Moving Marmoset Monkeys

Martin Lombard – CID: 01775468

Supervisors: Prof. Tim Constandinou, Dr. Ian Williams

Affiliated: University of Newcastle

Word Count: 5997/6000

Figures & Tables Count: 20/20

Abstract

Closed-loop auditory stimulation (CLAS) has become a promising method to modulate brain activity and could be used to target psychiatric disorders linked to the amygdala fear network. This Master's project presents the development of a high-performance neural logger designed for CLAS experiments in free-moving marmoset monkeys. The aim was to create a head-mounted device capable of local recordings and low-latency wireless transmissions while minimising the welfare impact on the animal.

A holistic approach encompassing firmware, electronics and mechanical design was employed. The device integrates a Nordic Semiconductors nRF52840 microcontroller, an Intan RHD2132 analogue front-end, and SD card storage. Wireless transmissions are performed over Bluetooth Low Energy (BLE). The housing leverages 3D printing to optimise weight, durability and servicing ease-of-use.

A mechanical and an electronic prototype were developed, achieving simultaneous local storage and wireless transmissions of 16 channels, sampling at up to 750 Hz with sub-10 ms wireless latency. The device enables sub-30 seconds battery servicing, weighs only 11.05 grams and measures 25.2 x 38.1 x 20 mm, significantly improving upon existing marmoset neural loggers. The device autonomy is an estimated 2 hours and 40 minutes using an 80 mAh battery at 500 Hz sampling rate per channel.

The developed logger represents an advancement in miniaturisation and functionality for small non-human primate neuroscience research. Its minimal animal impact could enable more naturalistic behavioural studies and offer novel flexibilities in experimental design, contributing to the development of psychiatric treatments leveraging non-invasive auditory stimulation.

1. Introduction

This Master's project is part of a collaborative neuroscience study between the University of Newcastle and Imperial College London. While the primary focus of this work is on the technical development of supporting hardware, understanding the broader context is crucial for appreciating the project's significance and goals.

Closed-loop auditory stimulation (CLAS) has long been proven to modulate brain activity non-invasively (1,2). Some frequency patterns introduced into the auditory cortex through sound can travel and affect other existing brain activity for potentiation and suppression, depending on their phase (3,4). This effect is well-proven enough for companies such as Elemind (5) or Neudio (6) to leverage it for sleep or general mental well-being.

Such modulatory effects depend on neurological networks linking auditory brain regions with the target region. The modulation target of this collaborative study is the amygdala, which features neurological pathways with the auditory cortex and the medial prefrontal cortex (mPFC) (5). Recent research has shown that fear acquisition and expression rely on the coordinated activity between the mPFC and the amygdala, with oscillations in the theta range (4-8 Hz) playing an essential role in inter-regional communication of the fear network (6). Notably, this coordination exists across animal models and humans (6-8). The amygdala, the brain's "emotional centre", is involved in many mental health disorders such as anxiety (9-11), and it presents a psychiatric treatment target, adjusting its mPFC-coordinated fear processing via non-invasive auditory stimulation.

This collaborative study aims to test the hypothesis that CLAS, aligning with mPFC-amamygdala circuit oscillations, can increase or decrease their activity and regulate cognitive control. In pursuing this objective, marmoset monkeys were selected as a model. This choice was motivated by their smooth brain topology, making electrophysiological readings easier to perform than for other primates (12,13). Moreover, the marmoset model is trainable and easy to handle thanks to its small size (350-400g), making it attractive for behavioural studies (13,14). Lastly, marmosets exhibit complex social behaviours, including diverse communication calls, which may increase their receptiveness to auditory stimuli (13,15,16).

Based on this context, this project aims to develop a device capable of emitting and storing invasively monitored live neural data from marmoset monkeys. The system should implement crucial principles in the literature to overcome challenges in device weight, ergonomics, ease of use, data throughput, and latency. After exploring existing solutions and defining design goals, this paper proposes a complete system across firmware, electronics and mechanical components. Next, prototypes are built and tested against original specifications. Additionally, tests are conducted to gauge the system's operating times. Lastly, the implications of this work, as well as its limitations and future developments, are discussed.

2. Background & Literature Review

2.1 Neural Loggers

Neural loggers are devices which record brain activity. Non-invasive methods, while less intrusive, suffer from lower spatial resolution, greater susceptibility to motion artefacts, and unsuitability for freely moving animals due to skin electrode limitations. Given these constraints and the need for freely behaving animal models in neuroscience (17), recent research in electrophysiology loggers has focused on developing lightweight, small, and efficient invasive devices (18,19). These implanted systems typically pre-process data before storing or wirelessly transmitting it for later analysis or real-time monitoring (*Figure 1*) (18,20,21). The challenges these devices face are related to the quantity and quality of the data, which are in trade-off relationships with respect to their dimensions (22). This makes their development a highly multidisciplinary endeavour across firmware, electronics and mechanical considerations.

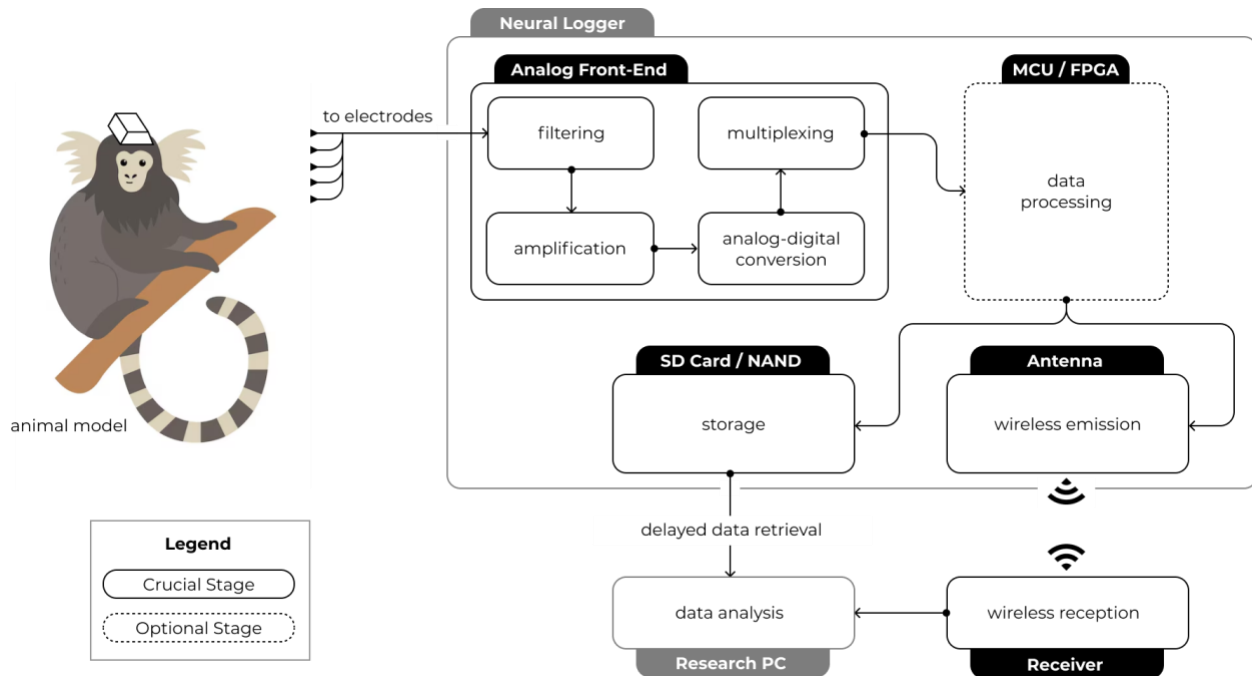


Figure 1: Typical neural logger data flow stages

Recent progress in miniaturised electronics has allowed for the introduction of ultra-small, wireless, battery-powered systems. These advancements have enabled a wide range of novel experimental setups, including long-term sleep studies in natural environments (23), monitoring of animals in social settings (24, 25), and even recording pigeons during flight (26).

2.2 Transmission Modalities

Whilst wired devices were historically favoured and are commercially accessible (27–34), wireless devices are prevalent today. In this branch, digitising neural signals before emission is an important consideration. The weight and power consumption needs introduced by analogue-digital converters (ADC) or microcontroller units (MCU) can make them burdensome (35). Thus, some studies emit raw analogue signals (41,42); Roy et al. (36) monitored marmoset monkeys via a wireless transmitter connected to electrodes. While this allowed them to bring the device's weight down to 12 g, transmitting analogue signals is noisy, necessitates RF/EMI shielding, custom receivers, and does not benefit from error correction methods through digital transmission protocols (16,36). Nowadays, most recent neural loggers' studies leverage digitisation before emission (25,33,35,37–39).

Continuous miniaturisation of CMOS (Complementary Metal-Oxide-Semiconductor) technology has led to substantial reductions in power consumption of digital circuitry, enabling complex onboard processing without sacrificing autonomy. These advancements have allowed larger, advanced commercial setups enabling 96 channels sampled at 30 kS/s wirelessly (40) and state-of-the-art ultra-small research loggers supporting 16 channels sampled at 19.5 kS/s (22). These findings strongly support the development of a device emitting digital wireless signals.

The choice of wireless transmission protocol is also crucial. It directly impacts the device's power consumption, throughput, and range. Several protocols have been used for neural recordings; in some of the smallest loggers, such as TaiNi, the analogue signals are digitised, multiplexed and emitted directly through custom protocols (22,41). While they can provide high throughputs at low-power consumptions, they require complex receivers with closely located antennas (22,41). To mitigate this, other systems have

leveraged 2.4 GHz communication links using commercial protocols such as Nordic Semiconductor's ShockBurst (23).

Alternatively, research systems utilised Bluetooth Low Energy (BLE) to emit data (21,37,39,42,43). BLE is advantageous as it does not require specialised receivers and is ubiquitously supported. Recent developments such as Bluetooth 5.0 introduced a 2 Mbps physical layer (PHY) and increased link range up to four times higher without raising output power (44), enabling new bio-logging setups.

2.3 Data Acquisition and Storage

Neural signals require pre-processing due to their low amplitude in the millivolt to microvolt range and various frequency bands of interest. While local field potentials (LFPs) are in the 1-300Hz range, action potentials (APs) are in the 300Hz-10kHz band (45). This segmentation and the wide dynamic range call for specialised analogue front-ends to perform amplification, filtering, and digital conversion (46).

These front-ends typically employ different strategies for Local Field Potentials (LFPs) and Action Potentials (APs). For APs, high-pass filtering is applied before amplification, allowing for high gains (1000-10000) without saturation. LFPs, however, require low-pass filtering and modest amplifications due to their larger amplitude fluctuations and low-frequency components. Analog-to-digital converters (ADCs) usually offer 10-16 bit depth, accommodating both signal types. Input-referred noise is a critical parameter, typically aimed below 10 μV_{rms} to ensure high signal quality (33,47,48).

In the literature, advanced systems use application-specific integrated circuits (ASIC) for analogue-digital conversion and multiplexing; this increases control over the pre-processing and can constitute small, lower-power solutions at the cost of expensive and longer developments (22,33,47,49). Alternatively, performant, off-the-shelf, low-power chips like the Intan RHD2000 series are widely used across research neural logging devices (12,23,43,46,50-52).

Once signals are digitised, they must be stored. While wireless emission and off-board storage are preferred for very light systems (22,37,39,41,53), this approach can limit autonomous recordings (18,23). To address this, loggers incorporate onboard non-volatile memory. The choice of storage technology involves careful consideration of capacity, complexity, and integration. NAND solutions like SD cards offer built-in controllers handling memory management. Although PCB-soldered NAND chips are common (20,21,42), SD cards prevail (18,23,26,46,54,55). They are easily replaceable, standardised, do not need weighty data ports, and offer built-in wear levelling. However, they require careful designs, as their memory architecture introduces variability in read/write times (21,56,57). Alternative options like eMMC offer similar benefits, but with permanent mounting, they may also require more complex interfaces and have capacity limitations.

2.4 Power Management and Battery Technologies

The choice of battery technology is crucial in wireless neural loggers, as the devices' dimensions, geometry, circuit design, and autonomy come directly downstream from it. Research loggers use various chemistries, including Zinc Air (22) and Lithium (20,23,35,37). Battery life can be measured in days in ultra-low power systems or larger animal devices (21,46). To understand miniaturisation trade-offs related to energy density, various chemistries and their form factors are compared in Table 1.

Table 1: Comparison of small battery technologies

	SR44W (58)	LR41 (59)	CR1225 (60)
Chemistry	Silver Oxide	Alkaline	Lithium Manganese Dioxide
Length (mm)	-	-	-
Diameter/ Width (mm)	11.6	7.9	12
Height (mm)	5.4	3.6	5.4
Weight (g)	2.2	0.6	0.9
Capacity (mAh)	165	32	48
Voltage (V)	1.55	1.5	3
Gravimetric Energy Density (mWh/g)	116.3	112.5	160
Volumetric Energy Density (mWh/cm³)	448.14	382.52	509.3
	ZA13 (61)	LP301013 (62)	LPM1254 (63)
Chemistry	Zinc-Air	Li-Po	Li-Ion
Length (mm)	-	13	-
Diameter/ Width (mm)	7.9	10	13
Height (mm)	5.4	3	6.5
Weight (g)	0.8	0.46	1.5
Capacity (mAh)	290	25	60
Voltage (V)	1.5	3.7	3.7
Gravimetric Energy Density (mWh/g)	543.8	201.1	148
Volumetric Energy Density (mWh/cm³)	1643.43	237.18	257.31

Zinc-Air and Lithium chemistries have high gravimetric energy densities. However, lithium-powered systems are more accessible to build, as Zinc-Air voltages are lower and require step-up converters to power traditional 3V components. Moreover, the power density of Zinc-Air batteries is limited, and they can fail if exceeded (61,64,65).

2.5 Miniaturisation

The miniaturisation of neural loggers minimises the impact on animal subjects. Key strategies have emerged to achieve compactness. Firstly, advanced systems combine multiple functions in a single ultra-compact IC. For example, TaiNi measures 20 x 12 x 14 mm (24). Similarly, Borna et al. conceived an ASIC with RF modulation and amplification functions to record cockroaches (49).

For systems requiring onboard storage or processing, PCBs are often split into different functions and stacked vertically to reduce footprints. In this arrangement, header pins channel power and information vertically to other boards (20,23,35,41,53,66). Beyond area reductions, this enables modular systems, where the SD card storage board is replaceable with a wireless board (12,23). Alternatively, others leveraged flex-rigid PCBs with connections between boards provided by flexible traces (46). Lastly, speciality micro-connectors, such as Omnetics, are ubiquitous in the literature (12,22,23,67).

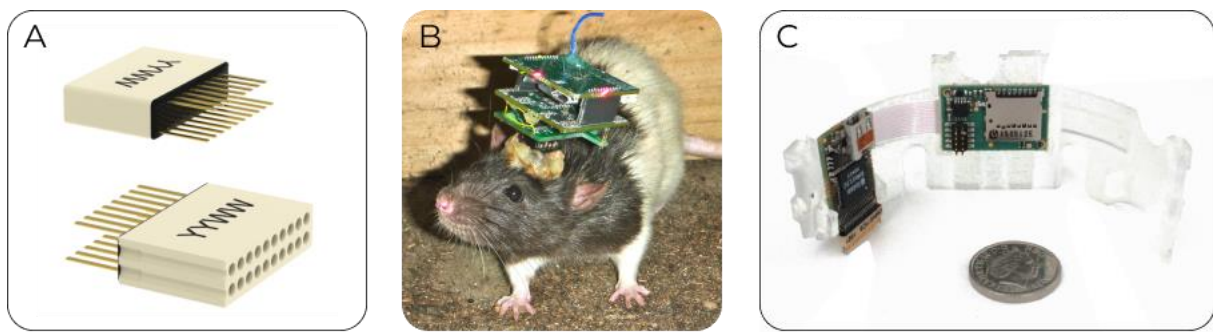


Figure 2: Examples of miniaturisation methods from the literature. (A) Omnetics micro-connector (68) (B) Rodent Scope system with stacked boards (35) (C) Compact recording platform for neural recording with real-time spike sorting, flex-rigid PCB (46)

2.6 Mechanical Design and Monkey Considerations

Whilst the electronic design of neural loggers allowing small animals to move freely is essential to their performance, the mechanical housing is an under-considered aspect. This is likely due to the focus of electronics engineers and the prevalence of rodents in science (69,70). As mice are smaller and less mobile than primates, rodent systems are uncovered and “stick out” (20,22,35,43,51,71,72). In monkeys, however, loggers must be protected against the animal’s inquisitiveness and forces they can induce (19,73). This protection is crucial for scenarios ranging from accidental impacts to social interactions, particularly in long-term recordings. Anecdotally, during a visit to Newcastle University, I witnessed an accidental fall of a marmoset; this reinforced the importance of well-protected systems.

The general maximum weight guideline for a head-mounted logger is 10% of the animal’s weight (74). However, ideal targets should be lower, as large loads negatively impact animal welfare and the quality of scientific results (22,36). With these constraints and primate-specific considerations, the housing presents an under-utilised weight reduction potential. The literature substantiates this interpretation. Multiple studies leverage crude cuboids to house the electronics (36,75), with large weights, reaching over 100 grams (38), wildly higher than the 1.5 grams of the smallest rodent logger (22), despite offering similar performances.

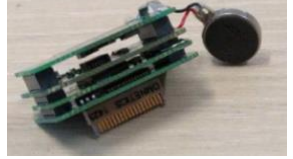
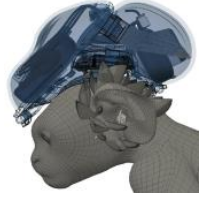
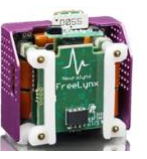
To address these challenges, recent studies leveraged 3D printing (12,46,75). This additive manufacturing method allows complex parts manufacturing with increased design flexibilities through light and durable polymers. This way, PCBs can be protected with minimal material volumes. For instance, Walker et al. (12) developed a modular 3D-printed logger housing for marmosets, incorporating easily replaced

batteries. This modular approach addresses the need for various autonomy levels and improves usability by facilitating battery swaps, enhancing animal welfare by reducing immobilisation times (19).

2.8 Taxonomy of Existing Solutions

To summarise the research and commercial device landscape, Table 2 below presents a few wireless neural loggers for free-moving animals.

Table 2: Comparison of research and commercial small-animal neural loggers

	TaiNi (22)	ONEIROOS (23)	Chronic Wireless Recordings w/ Marmosets (12)
Image (from reference)			
Context	Research	Research	Adapted Commercial Device
Wireless Transmission (GHz)	2.3	2.4	3.05 OR 3.75
Local Storage	-	Wireless OR Local SD Card	-
Dimensions (mm)	20 x 12 x 14	28 x 18 x 15	37.2 x 73 x 41.2 (full assembly)
Weight (g)	1.5	5.5 (without enclosure)	24
Autonomy (hrs)	72	24-100	4
Channels	16	26	96
Sampling Rate (kS/s)	19.5	0.3 (max per channel)	30
Notable Shortfalls	Requires complex antenna setup. Wireless latency unspecified.	No simultaneous local storage and wireless emission. Sampling rate is low. Wireless latency unspecified.	Remains very heavy (~6.5% of animal weight) and does not allow for local storage. Wireless latency unspecified.
	MouseLog16C (55)	FreeLynx (54)	Implantable Neurophysiology Platform (63)
Image (from reference)			

Context	Commercial	Commercial	Research
Wireless Transmission (GHz)	-	5 (Wi-Fi)	2.4 (BLE)
Local Storage	SD Card	Wireless OR Local SD Card	Local NAND Chip
Dimensions (mm)	13 x 18 x 10	30 x 35 x 30	20 x 20 x 10
Weight (g)	2.88	21.3	8.5
Autonomy (hrs)	1.6	24	84
Channels	16	64	4
Sampling Rate (kS/s)	31.25	30	0.125
Notable Shortfalls	No wireless transmission. Relatively low autonomy.	No simultaneous local storage and wireless transmission. Relatively heavy package. Wireless latency unspecified.	Low channel count and low sampling rate for a relatively heavy package. Wireless latency unspecified.

2.9 Ethical Considerations

The use of marmoset monkeys in this research demands robust ethical considerations. While the Newcastle University manages animal sourcing, surgeries, and handling, Imperial's ethical responsibility lies in developing a device minimising invasiveness and maximising welfare throughout its lifecycle.

The primary ethical focus is minimising the head-mounted device's impact on marmosets, with volume and weight as crucial factors. Careful engineering must balance mechanical objectives with data acquisition goals. Secondary considerations include reducing "head fixing" duration and frequency for maintenance and data offloading and implementing teleoperation to minimise animal immobilisation. The design should prioritise ease of use for researchers, indirectly benefiting animal welfare by reducing errors, shortening handling times, and minimising stress (76). This often-overlooked ergonomic aspect is crucial in animal research equipment (77). These considerations align with producing more reliable results, as motility constraints can modify marmoset behaviour (36). Thus, reducing the device's impact on animal behaviour is both an ethical and performance objective.

This research's ethical implications extend beyond immediate animal welfare. The development of miniaturised neural loggers, as seen in TaiNi (22) and ONEIROUS (23), reflects a trend towards sophisticated brain-computer interfaces, raising societal questions about privacy, augmentation, and technology neutrality. Environmentally, miniaturisation and battery efficiency align with sustainability goals, potentially reducing electronic waste in long-term studies. However, these specialised devices pose recycling challenges, dampened by low production volumes. Economically, while initial research costs are high, successful developments could lead to more cost-effective neuroscience research and accessible human treatments. The research's potential for developing non-invasive psychiatric treatments through auditory stimuli, coupled with insights into neurological mechanisms related to autism and sleep, offers a favourable risk-benefit ratio. This aligns ethical goals with potential applications in human healthcare, benefitting the public and enhancing Imperial's reputation in neurotechnology.

3. System Specification

Neural loggers have become essential in neuroscientific studies, with trends pushing towards improved communication protocols, ASICS, and reduced animal disturbances. However, many solutions still fall short of ideal mass and dimensional targets, particularly for primate research. Housing configurations often add unnecessary weight, flexibility is limited between local storage and wireless transmission, and modularity with rapid battery changes remains an unmet ethical need.

Based on this analysis and the collaborative study requirements, there's a gap for a highly miniaturised neural logger for marmosets with optimised housing, improved usability, and functional flexibility. Key development objectives are outlined in *Table 3* below.

Table 3: System specification

Code	Name	Value	Description
E1	Autonomy	2 hrs - ideally 24 hrs	The study's maximum license-allowed recording time is 2 hrs. To enable the system's extended use beyond this research, higher recording times are desirable.
E2	Channel Count	≥ 16	16 channels are necessary as the electrodes inserted in the marmoset's brain have 16 contacts.
E3	Sampling Rate	100 Hz/channel – 10 kHz/channel	LFP recordings are sufficient for the study. Ideally the logger should support AP recordings.
M1	Dimensions	40 x 70 x 40	The device must be as small as possible. Dimensions should be comparable to the latest marmoset research.
M2	Weight	40 - 12 g	The device weight must be under 10% of the monkey's weight, which is around 40g. Ideally, lighter than the best marmoset logging research (12g).
M3	Durability	High	The device should sustain accidental damage from monkey behaviour.
P1	Wireless Range	$\geq 5\text{m}$	Based on the enclosures at Newcastle University, the operating range of the device should be above 5m.
P2	Latency	< 10 ms	The signals are highly time sensitive for CLAS and should reach the receiver in under 10 milliseconds.
P3	Local Storage & Wireless	Yes	The device should be able to simultaneously record brain activity locally and emit it to research PCs.
D1	Plug-&-Play	Under 2 min	The headstage and battery swaps should be made to be very fast to operate.
D2	Remote Operation	Yes	The device should be able to switch modes without requiring the immobilisation of the animal.

4. Methods

4.1 System Design

The system's design was planned before engineering developments, with development principles such as an iterative approach and minimising components, being integral to the process (Appendix: Figure 17). The process had to be adjusted due to administrative and manufacturing delays related to the financing and ordering of the PCB. Consequently, an electronics-firmware prototype and a mechanical prototype with mock PCBs had to be built. The firmware and "breadboard" electronics prototype were developed first to reduce risks using the selected components and to guide the housing design.

Early considerations were made with Newcastle University to ensure continuity with their systems (Appendix: Figure 18). For example, allowing the electro-mechanical system to connect to their "crown", an electrode housing permanently cemented to the monkey's skull, enabling the monkey's head fixation, and ensuring compatibility with Omnetics connectors used within the crown.

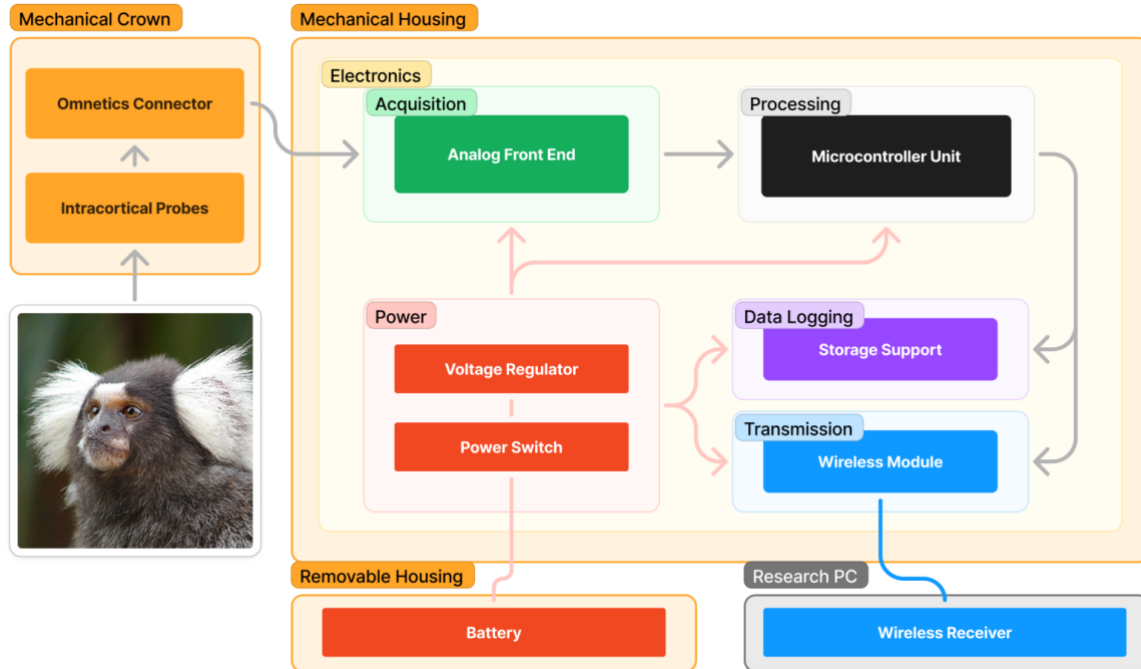


Figure 3: High-level system architecture

The high-level system architecture (Figure 3) illustrates the neural logger's key components and data flow. The system is divided into three main parts: the Mechanical Crown, the Mechanical Housing containing the active electronics, and the Removable Battery Housing. This separation enables battery replacement and maintenance without disturbing the animal or sensitive electronics. This architecture addresses specifications P3, D1, and D2. The Modular design also facilitates future upgrades and modifications to create a flexible, researcher-friendly device while minimising animal impact.

4.2 Electronics & Firmware Development

4.2.1 Electronics Development

Microcontroller Unit Selection

The core components were selected based on the system design. The MCU selection focused on low power consumption, SPI interfacing, integrated antenna modules, firmware development environment, and customer support. The Nordic Semiconductors nRF52840 was chosen for its ultra-low power consumption, 64 MHz ARM Cortex-M4 processor, Bluetooth 5.0 support, sufficient memory for SD card buffering, multiple SPI interfaces, robust development platform, and availability in compact modules with built-in antennas.

BLE 5.0, supported by the nRF52840, was selected as the wireless link. Its 2 Mbps physical layer theoretically provides throughput up to 7812 S/s for 16 channels sampled with a 16-bit depth, exceeding the ~30 S/s needed to acquire CLAS's targeted theta waves (4-8 Hz).

Following the MCU selection, two modules with integrated antennas were compared (Appendix: Table 5). The ISP1807 module was selected for its very low size and comparably low power consumption during transmitter use.

Storage Support Selection

Several storage options were considered, including on-chip flash, eMMC, and SD cards. After evaluating options, an SD card was selected (Appendix: Table 6). It allows for easily expandable capacity, removability to offload data without extra ports, heightened ease of use, and SPI compatibility with the MCU.

Analog Front-End Selection

The Intan RHD2132 was selected as the analogue front-end after considering five main options, including the RHD2116, TI ADS1298, ADS1299, and a custom op-amp-based solution (Appendix: Table 7). The RHD2132 was chosen for its high channel count allowing future expansion, high sampling rate, low power consumption, excellent noise performance, and small package size. While TI options offered higher bit depth, their increased power consumption and limited channel count made them less suitable. A custom op-amp solution was rejected due to increased development time and complexity.

Additional Components Selection

Power management was designed for minimalism and efficiency. A Li-Po **battery** was selected for its high energy density, peak power output and rechargeability. The LP5907 low-dropout **voltage regulator** maintains a stable 3.3V supply, balancing efficiency and low noise. A mechanical switch provides clear on/off indications. An **LED status indicator** was omitted to reduce weight and power consumption, as device status can be communicated via the low-latency BLE link. These choices contribute to a streamlined, power-efficient design prioritising essential functionality.

Circuit Diagram

The selected components come together in the circuit diagram below (Figure 4).

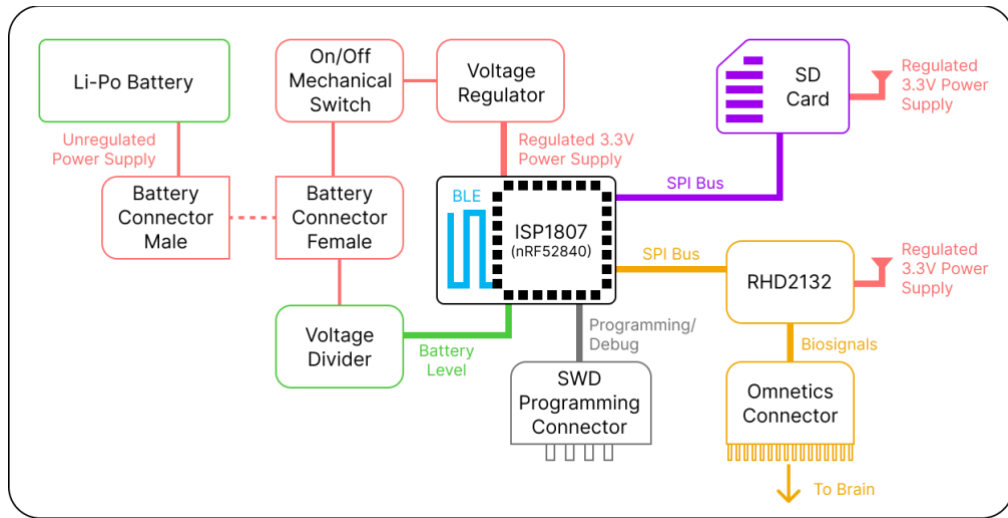


Figure 4: System Circuit Diagram

Breadboard Prototype

To support the device development, a “breadboard prototype” was built (Figure 5). It acts as a functional analogue to the system circuit with the same core components. It is built around the nRF52840 development kit (DK), with the DK offering its voltage regulator and switch. The prototype features a 3.7 V, 300 mAh Li-Po battery, an SD card breakout board, and an Intan RHD2132 supported by a zero-insertion-force connector (ZIF). A signal generator followed by a voltage divider simulates neural signals of the correct amplitude. While the prototype incorporates more components than the final design, likely resulting in higher power consumption, this setup provides a “worst-case scenario” for testing. Therefore, the final PCB is expected to yield improved results. This interim solution, necessitated by PCB manufacturing delays, enabled early firmware debugging, mitigating development risks.

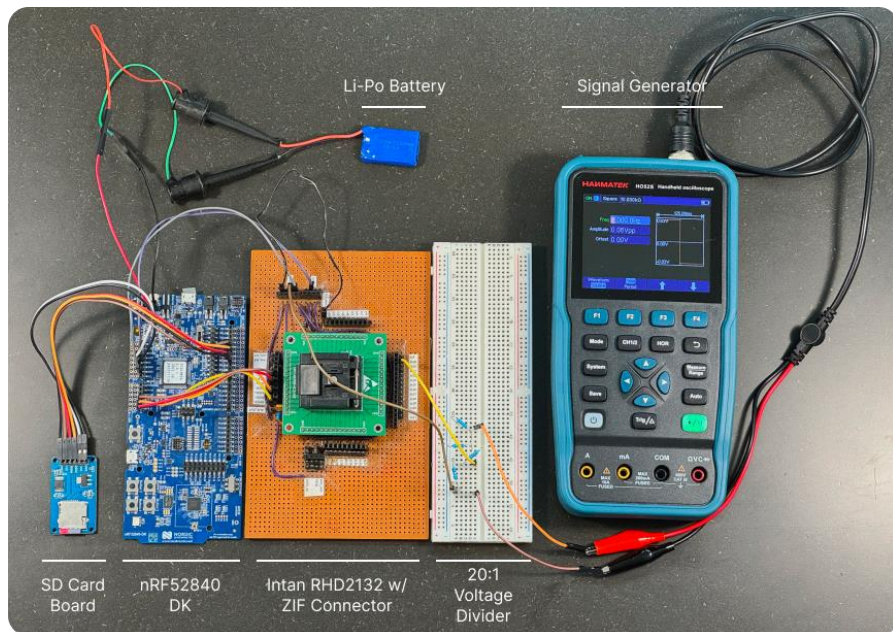


Figure 5: Breadboard prototype

4.2.2 Firmware Development

The latest firmware version follows an asynchronous multi-threaded design (Figure 6). Four main threads perform the Bluetooth device status, Bluetooth neural data, SD card, and RHD2132 sampling operations. The firmware is built around a circular first-in-first-out (FIFO) buffer, which stores the neural data and shares it across task threads.

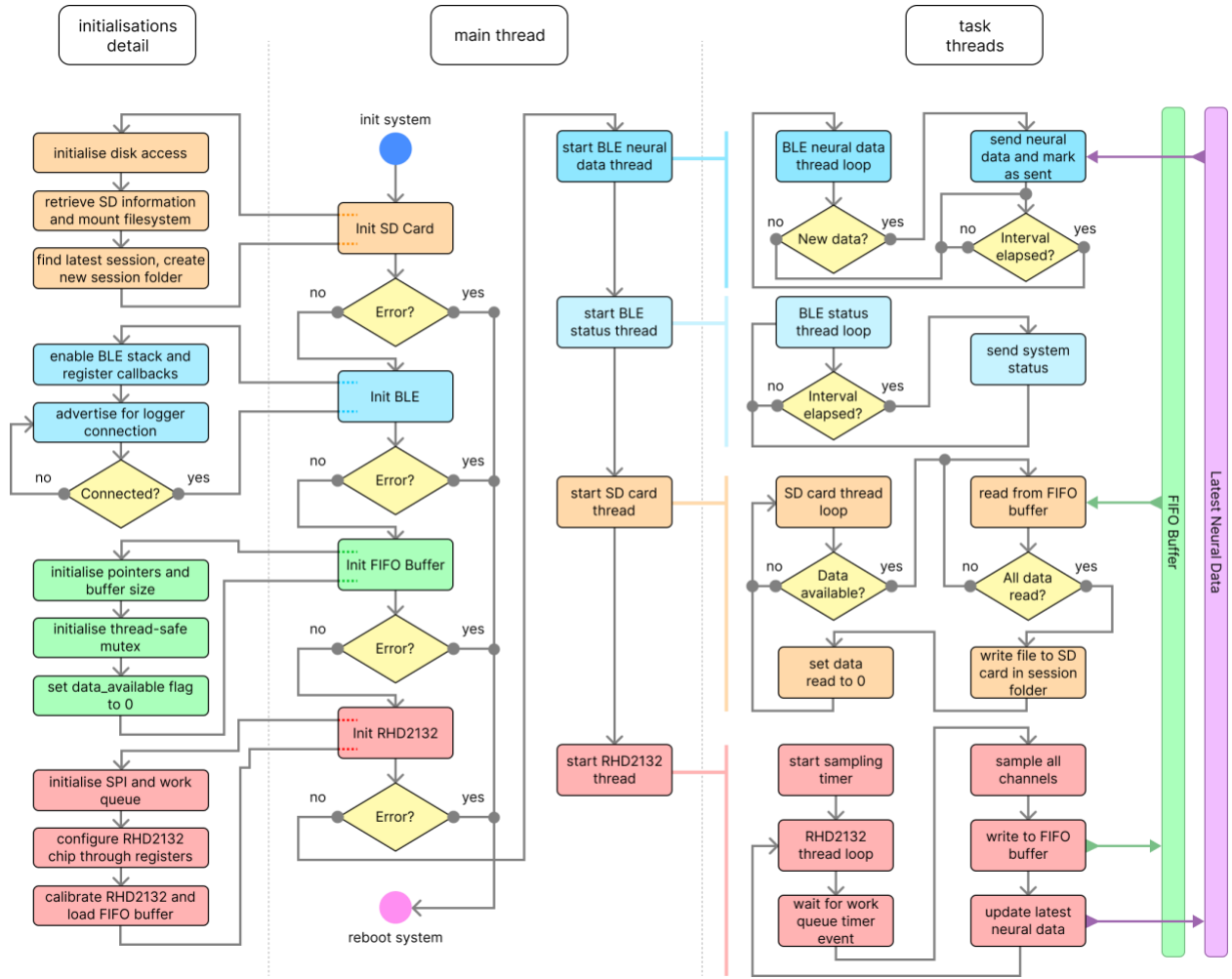


Figure 6: Firmware logic flow diagram

System Initialisation

The system is initialised by progressively running through hardware peripherals and ensuring appropriate responses. Beginning with the SD card, the disk access is started, and the card is mounted. Once the SD storage is initialised, the firmware finds the latest session folder with the highest number (e.g. session_21) and creates a new folder by incrementing it. This ensures the system autonomously stores each experiment separately at every boot without overwriting past data.

Then, BLE is enabled, and the logger advertises its connection availability. As soon as the system connects to the receiver, the connection callbacks negotiate the highest possible Maximum Transmission Unit (MTU) size of 244 bytes. They also enable the 2 Mbps PHY and set the lowest BLE connection interval of 7.5 ms, ensuring low latencies.

The FIFO buffer is then initialised. Following this, the RHD2132 SPI connection is verified, and the work queue is created. The RHD2132 is configured by writing to the on-chip registers. Every register write is checked for an appropriate response. If the initialisation fails, it is re-attempted up to five times before rebooting the system entirely if unsuccessful. Lastly, the RHD2132 performs an auto-calibration to finalise its initialisation.

Once all systems have been initialised, the task threads are started in reverse computational load order. This ensures no data is pre-loaded before the SD card thread starts, preventing early overloading.

RHD2132 Thread

The RHD2132 thread is responsible for the time-critical neural data sampling. It utilises a high-priority work queue to ensure precise timing in data acquisition. Once initialised, a kernel timer submits sampling work items to the queue at regular intervals.

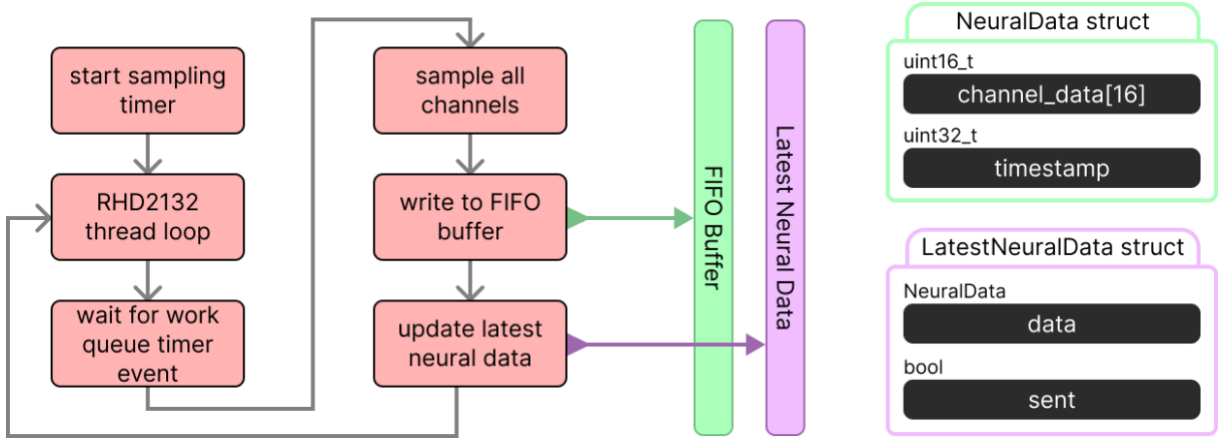


Figure 6.1: RHD2132 thread diagram focus (left), used data structures (right)

The data acquisition (Figure 6.1), performed by the RHD_handler function, samples channels using SPI transactions, formats data into a NeuralData structure, timestamps the data using the system uptime, and lastly, writes the data to the FIFO buffer and latest_neural_data for the SD card and BLE threads.

FIFO Buffer

The FIFO buffer is the software's data backbone (Appendix: Figure 19). It is implemented as a circular array of NeuralData structures, allowing continuous writing and reading without frequent memory reallocations. It utilises a mutex for thread-safe access, preventing data corruption. Moreover, a data_available semaphore signals when the buffer reaches 50% fill, optimising the SD card thread.

SD Card Thread

The SD card thread persistently stores the acquired neural data (Figure 6.2). The thread waits for data availability. It then reads data from the buffer in chunks of 128 NeuralData structures. This number was chosen as each NeuralData structure is 36 bytes long, bringing the total byte count per SD card operation to 4608, a multiple of 512, the fastest block size to write (57). The thread writes binary files into the current session folder with incremental naming (e.g. data_64.bin). A minor delay is implemented between writes to prevent tight looping.

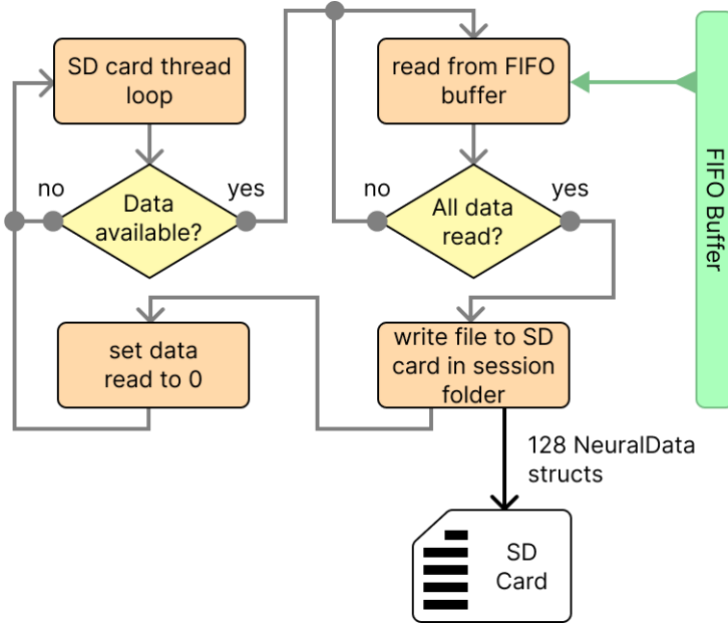


Figure 6.2: SD card thread diagram focus

BLE Service and Threads

Two BLE threads operate the wireless transmission of neural data and the device's status. They are built on a custom generic attributes (GATT) service named Neural Bluetooth Service (NBS) providing the two characteristics to be emitted (Appendix: Figure 20). Both characteristics offer client descriptors enabling notifications on the receiver side.

The BLE Neural Data thread (Figure 6.3) operates at a higher priority with a 1-ms check interval; it continuously polls for new data and notifies the receiver when data is available. After the emission, it marks data as sent to prevent duplicates. Given the BLE connection interval limitations, the thread manages data transmission at a rate suitable for the CLAS-targeted LFP frequencies. While this meets the requirements for wireless transmission of LFP data, the full-resolution data is safely stored on the SD card for comprehensive analysis. The status thread runs at a lower priority and updates every second; it emits status data information such as battery level, temperature, recording status and configuration.

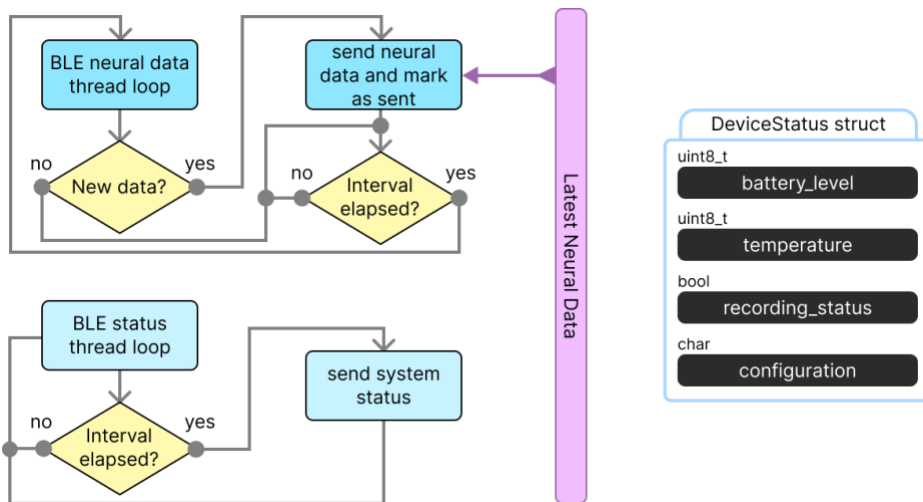


Figure 6.3: BLE threads diagram focus (left), DeviceStatus struct (right)

4.3 PCB Design Process

The PCB design was initiated once the components and firmware were validated through the breadboard prototype. First, components were laid out in 3D to understand their ideal placement over the crown (Appendix: Figure 21). In the final layout (horizontal), the RHD2132 is located as close as possible to the Omnetics connector to minimise analogue trace lengths. The MCU-antenna module is at the front, ensuring as little obstruction to the antenna as possible, as the head tissue (below) and metal SD card holder (above) are RF-blocking. Less sensitive components, such as the SD card holder and the power subsystem, are placed on the top board.

A stacked-boards approach was taken, as the components could not fit on a single small-area PCB. This was iterated to minimise manufacturing costs and shorten timelines, starting with a flex-rigid-PCB and settling for a stacked board assembly (Appendix: Figure 22), leveraging micro-header pins.

The final boards (Figure 7) have no mounting support holes and use micro-components where possible to minimise area. Moreover, through-vias are as large as possible to minimise costs. Lastly, the PCB's bottom board features soldering pads to short the reference, channel-1 and ground if necessary.

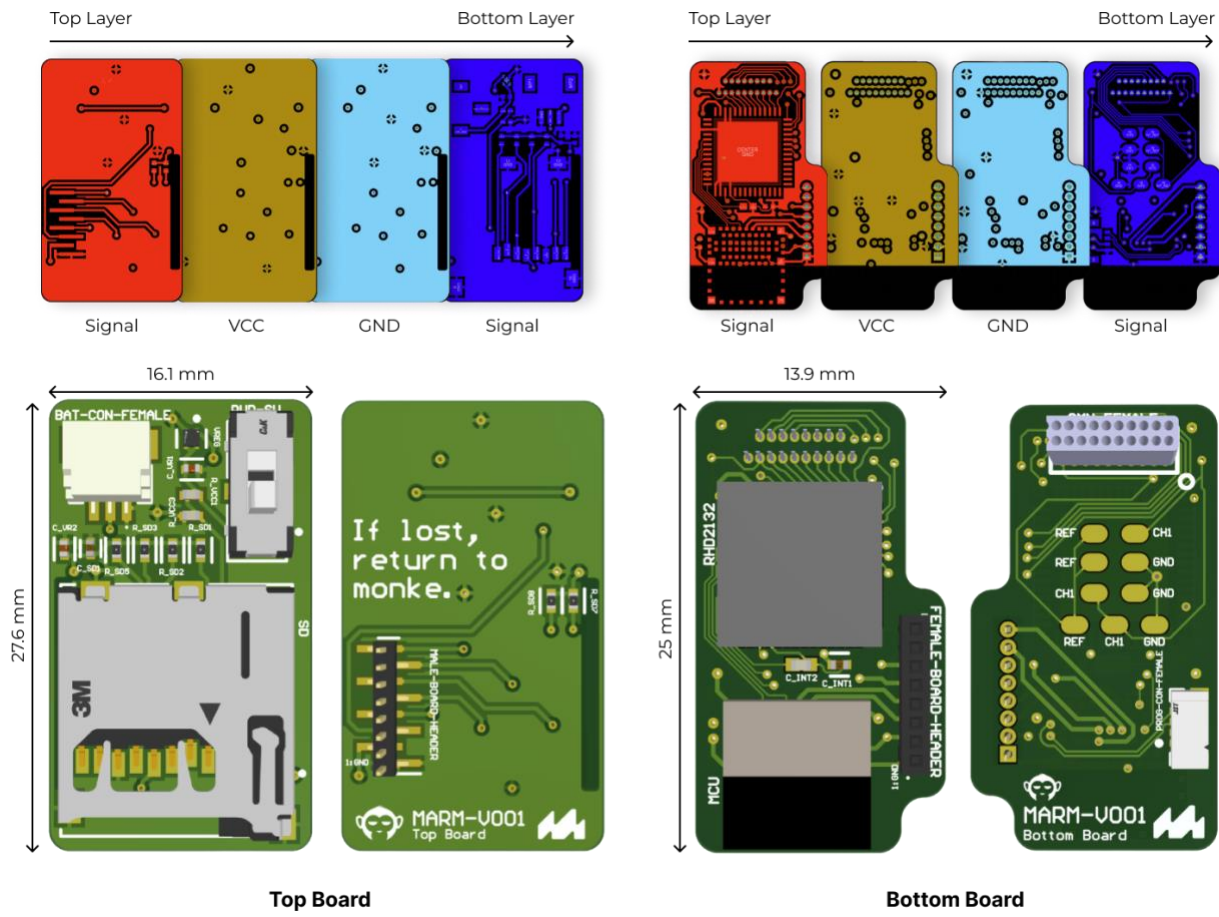


Figure 7: Final dual-board PCB

4.4 Mechanical Design

The mechanical design needs to fulfil the objectives of supporting and protecting the PCB, mating with the crown, being easily assembled, and providing an easily swappable container for the battery, all in a light format. Multiple part iterations were explored to achieve these goals (Figure 8). Each iteration was followed with FDM (fused deposition modelling) 3D-printing prototypes to test assemblies (Appendix: Figure 23).

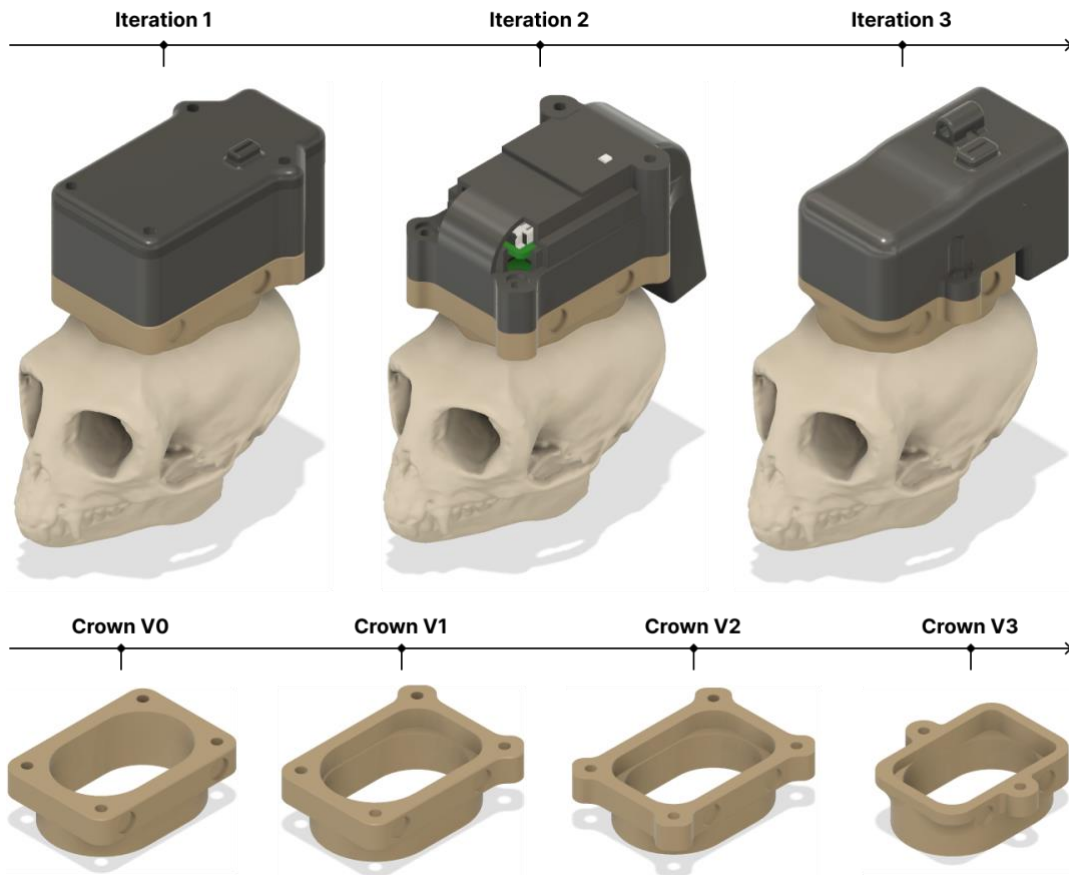


Figure 8: Mechanical design iterations

For the final housing parts and building on the literature, SLA 3D-printing was selected as the target manufacturing method. This allowed more freedom in the design to minimise weight. On the other hand, the crown is milled out of a high-performance polymer (PEEK) block. Newcastle's initial crown was also iterated on as it was unsuited to the PCB design; skull interface surfaces were left untouched.

Iterations 1 and 2

The first iteration (Figure 9) was built as an “exploratory” design to understand the PCB support geometry. Stacked supports constrain movements of the two boards in XYZ, and a holder houses the Li-Po cell. The design is relatively light and small (7.7g, 25.6 x 40.2 x 27.2 mm). However, it does not offer rapid battery replacements, as the entire stack needs to be disassembled. To overcome this, the second

iteration provides a cover, which only necessitates two screws to be removed. This induced a weight increase of ~0.8g compared to Iteration 1, with a bulkier design. On top of this, both iterations feature screws at the front within the metal exclusion zone of the MCU's antenna, which is sub-optimal for BLE range performance. The material selected for weight calculations is the final material, a translucent, high-strength, and biocompatible polymer (78).

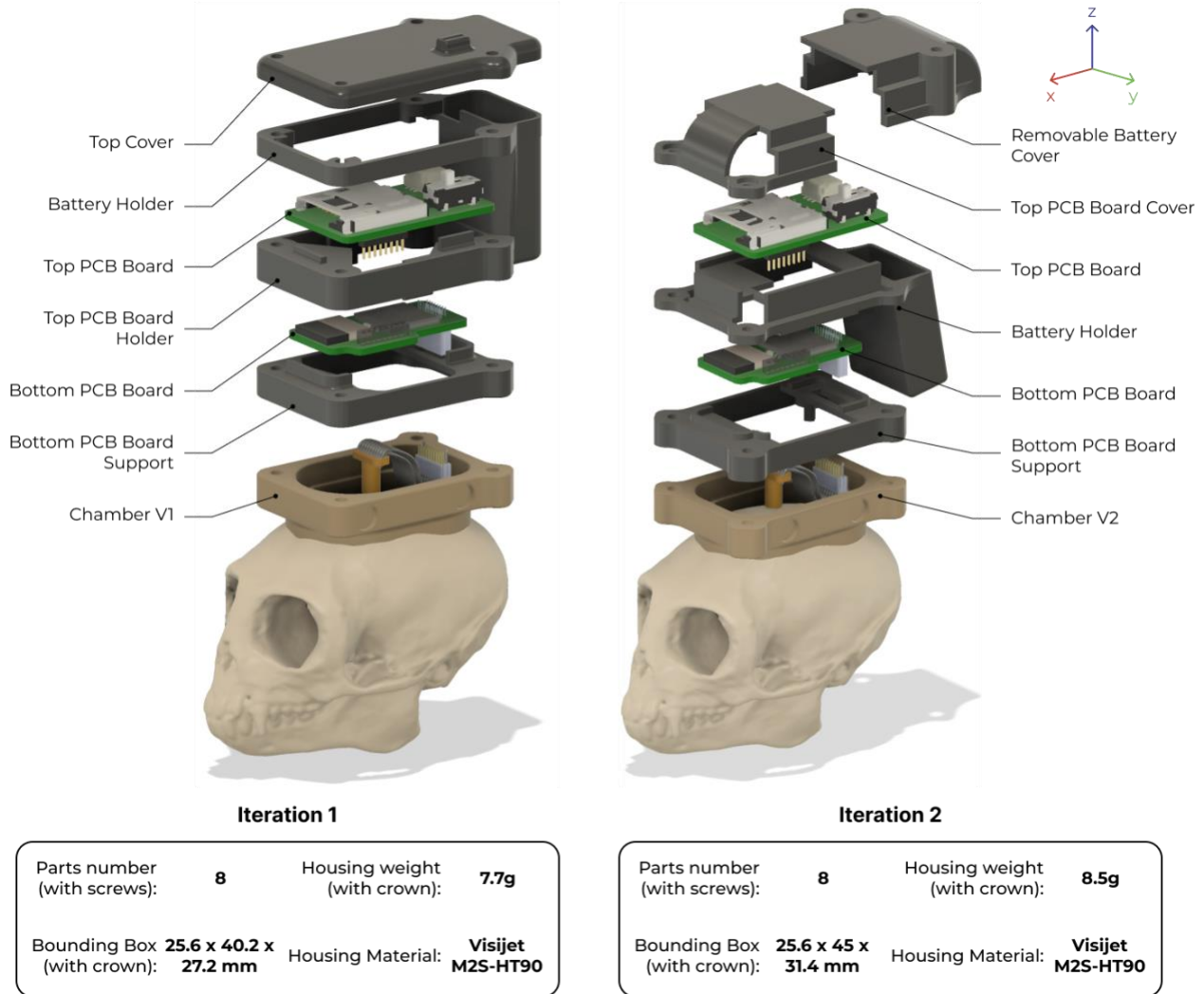


Figure 9: Housing design iterations 1-2

Final Design

The final design (Figure 10) builds on the previous iterations via a small and light form factor, with a quick-swap battery cover held by one screw. The design only needs two screws to separate it from the chamber. These are removed from the antenna's exclusion layer and shortened, eliminating further weight. Modifying the crown improved the design, which now provides internal shelving holding the PCB board support.

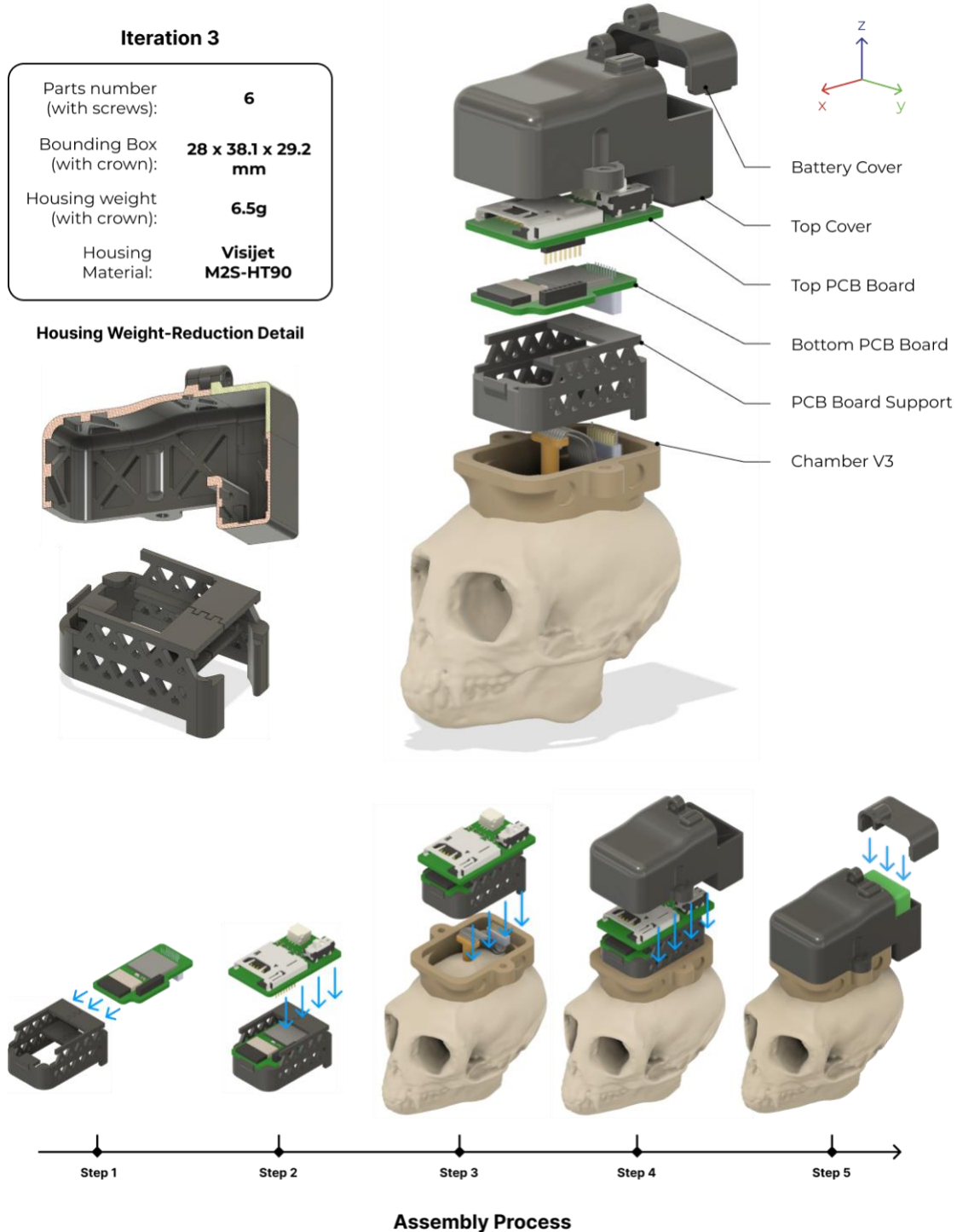


Figure 10: Housing final design (iteration 3), and assembly process

The number of parts is also reduced, facilitating assemblies with only one PCB support, constraining the bottom PCB board in XYZ, and supporting the top PCB board in Z. The top board is constrained in XY by the header pins, which don't undergo mechanical stress thanks to the top cover. Moreover, the design shaves off approximately 0.7g through wall cutouts in the top cover and PCB board support. The thinnest walls are 0.5 mm. Lastly, a thin cutout enables the operation of the mechanical switch whilst rendering it inaccessible to the marmosets.

5. Evaluation & Results

5.1 Electronics & Firmware Performance

Functionality

The breadboard prototype was tested for data acquisition. General functionality was validated by powering the prototype with a Li-Po cell and producing sinusoidal signals with a generator. The logger successfully recovered data over BLE through the nRFConnect BLE Desktop App. Moreover, a Python script was used to process and plot SD card data, further proving the device's functionality (Appendix: Figure 25). The prototype was also operated successfully with a wired power connection and continuous logging for 11.5 hours, sampling at 250 Hz. The logging was manually interrupted but performed as expected throughout.

Data Throughput

Data was recorded and compared with expected throughputs to evaluate performance at varying sampling frequencies (Figure 11). A fakedata generator thread was set up to separate the performance loss caused by the Intan RHD2132 thread from an “ideal” data source. The expected SD card performance is maintained up to ~750 Samples/s/channel with a throughput drop-off at higher frequencies and failure above 1200 Hz. The BLE link is more constrained, with earlier and more intense performance losses past 100 Hz.

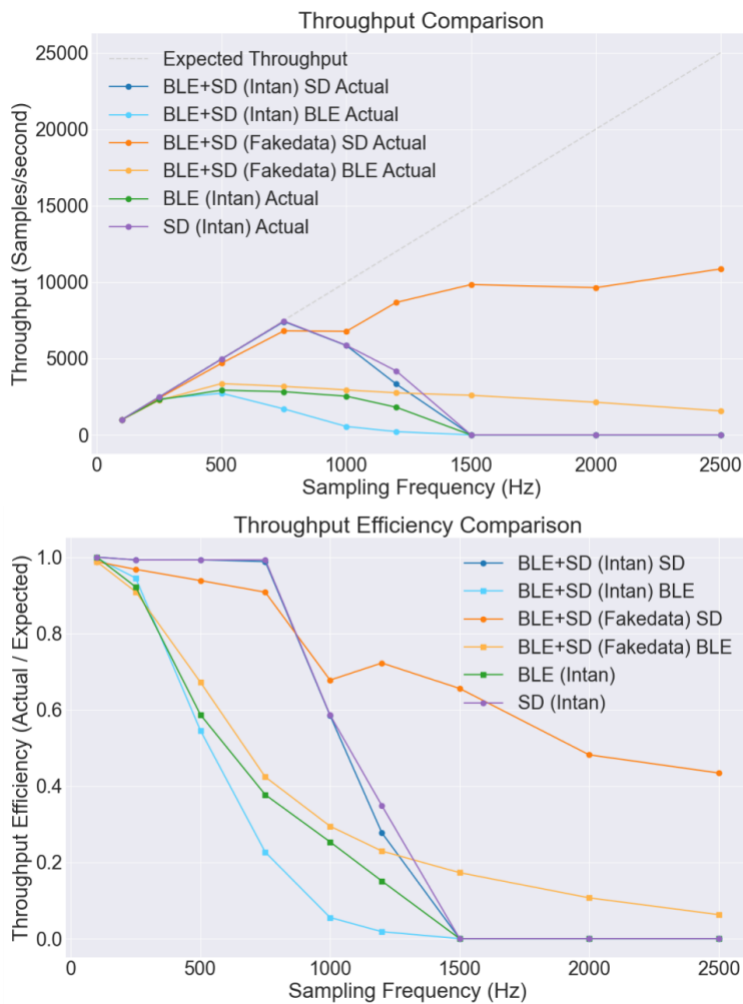


Figure 11: Throughput comparison (top), throughput efficiency (bottom)

In its standard mode (BLE+SD), the system stability is maintained up to 750 Hz for the SD card logs and 100 Hz for the BLE data logging (Figure 11 and Appendix: Figure 26). The stability metric is based on a maximum of 100 samples lost in a recording period of 10 seconds. These maximums remain the same for BLE-only or SD-only logging using the RHD2132.

Latency

The latency of the BLE link was evaluated by examining the deviations between actual and expected connection intervals across various sampling frequencies (Figure 12). This analysis is grounded in the principle that BLE data is transmitted exclusively on newly available “latest neural data” structures. Consequently, any deviation from the expected rate directly reflects the inherent latency of the BLE transmission process.

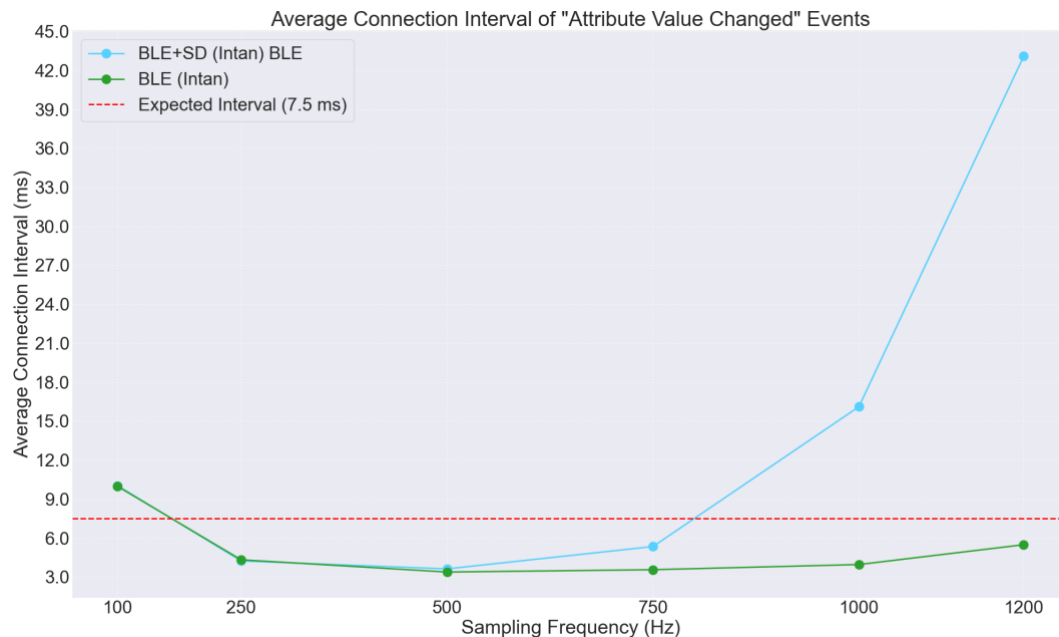


Figure 12: BLE connection interval at different sampling frequencies

Given the sampling frequency, the connection interval is expected to be 10 ms at 100 Hz. The interval is lower than the target value at higher sampling rates, indicating very low latency performance. This interval rises above the target at frequencies ≥ 1000 Hz in the BLE+SD experimental setup. It remains lower than the 7.5 ms target in the BLE-only setup, indicating the interval increases are likely due to resource constraints induced by the parallel SD card logging.

Power Consumption

The prototype's power consumption was analysed in different setups using the Agilent N6705B DC Power Analyser for a 2-second window, supplying the logger with 3.7 V whilst recording signals from the generator. The spikes in Figure 13 below correspond to SD card writing events, with lower amplitude spikes corresponding to periodic BLE emissions. The system overloads at 1000 Hz as the SD card writes are less frequent than at 500 Hz.

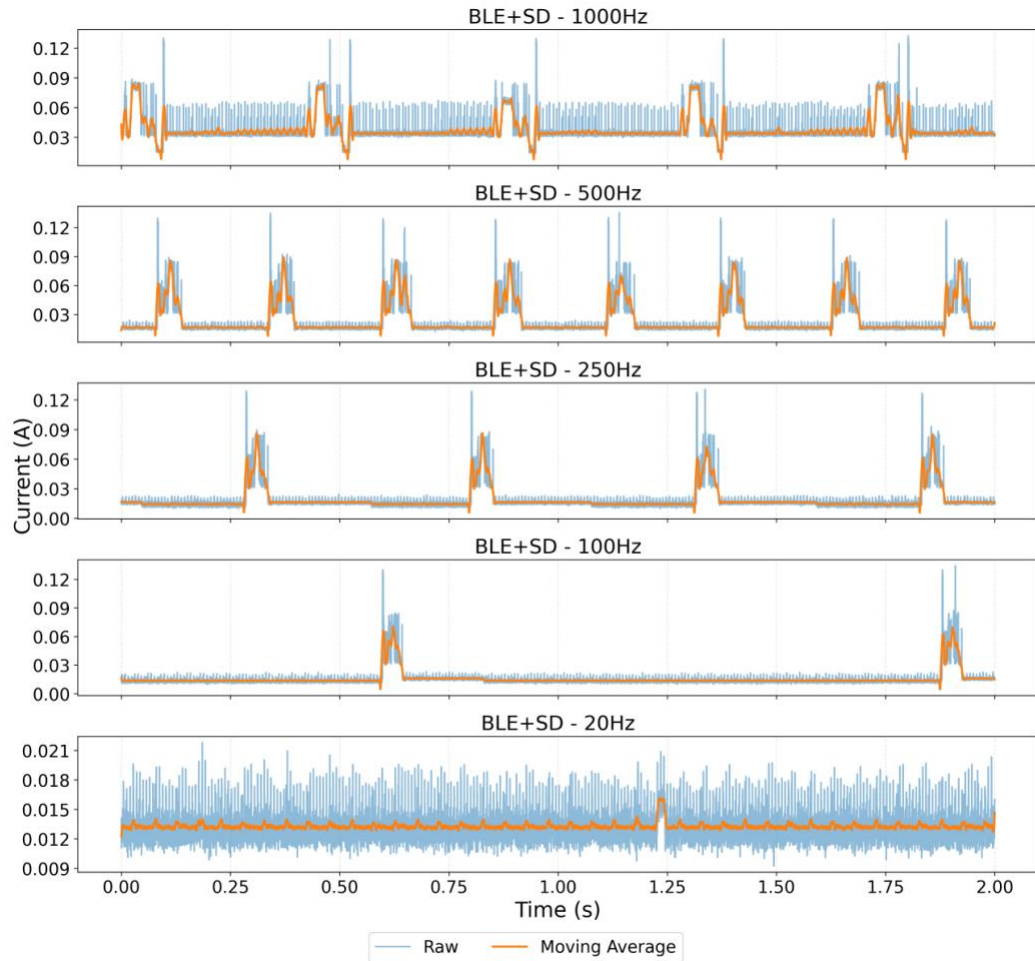


Figure 13: Device current for 2-second operation windows at different frequencies

Figure 14 presents the average power consumption for the device across various experimental setups and sampling frequencies. The BLE+SD configuration, combining wireless transmission and SD card logging, exhibits the highest power consumption, particularly at 1000 Hz, reaching approximately 37 mA. This elevated consumption at higher frequencies is driven by the increased data throughput, demanding more frequent SD card writes and continuous BLE transmissions. In contrast, the BLE-only and SD-only configurations show relatively stable power consumptions across all frequencies, with BLE-only peaking around 16.6 mA at 1000 Hz. This highlights the efficiency of the BLE connection compared to SD card operations, especially at higher data rates. The Idle state maintains a low consumption, around 12.9 mA.

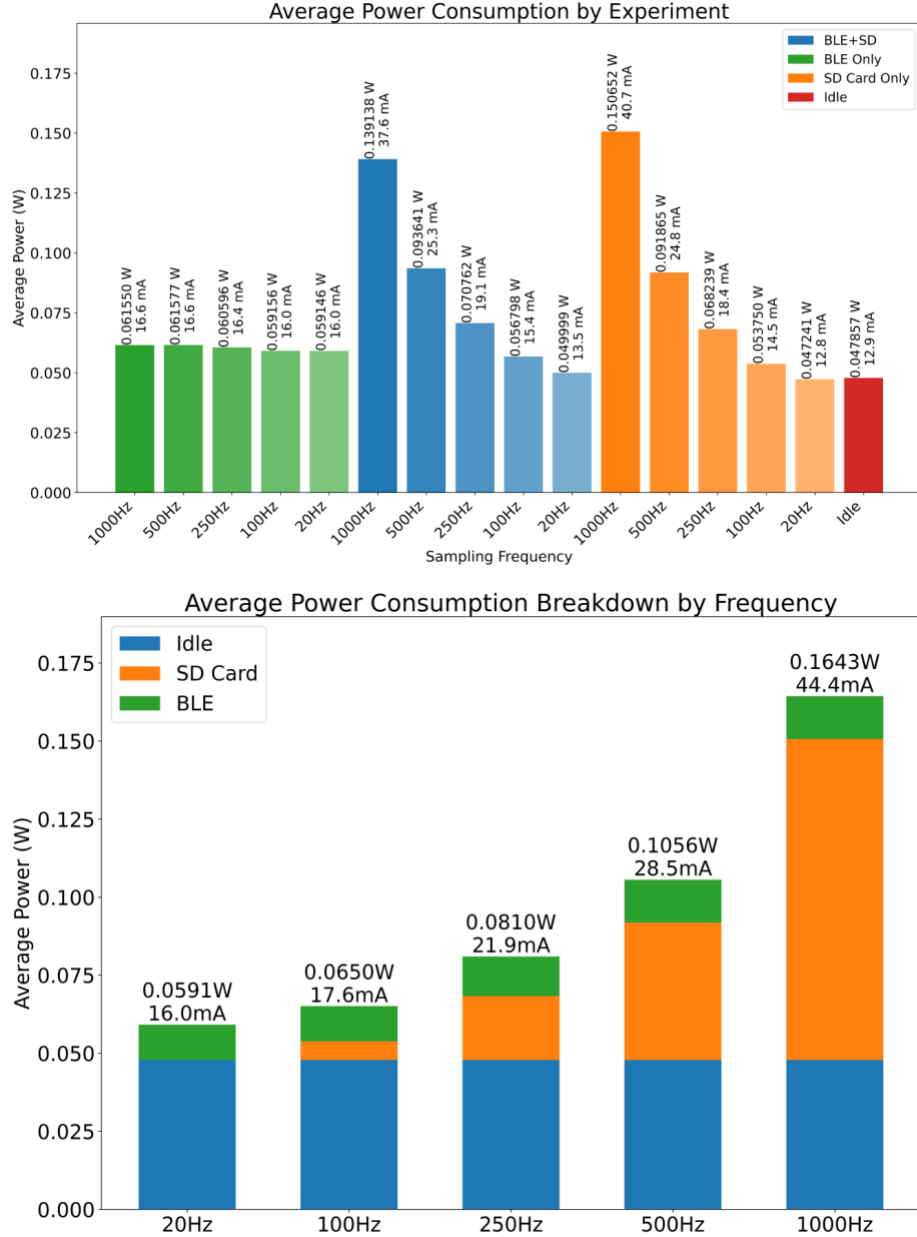


Figure 14: Average power consumption by experiment and sampling frequency (top), average power consumption breakdown by subsystem and sampling frequency (bottom)

The average power consumption for the highest tested stable sampling frequency (500 Hz) is around 30 mA. The consumption breakdown was calculated from the proportions of the total consumption using the individualised consumption experiments. The idle and SD card processes use most of the power consumption, with the BLE consumption remaining stable at higher frequencies. The average power consumption at 500 Hz would yield an autonomy of 2 hrs and 40 min with an 80 mAh battery.

5.2 Mechanical Design Outcomes

Dimensions & Mass

The final complete assembly, including the crown and the battery, totals 11.05 grams and measures 25.2 x 38.1 x 20 mm (Figure 29). The PCB mass was estimated conservatively by assigning aluminium to all components and FR4 to the boards.

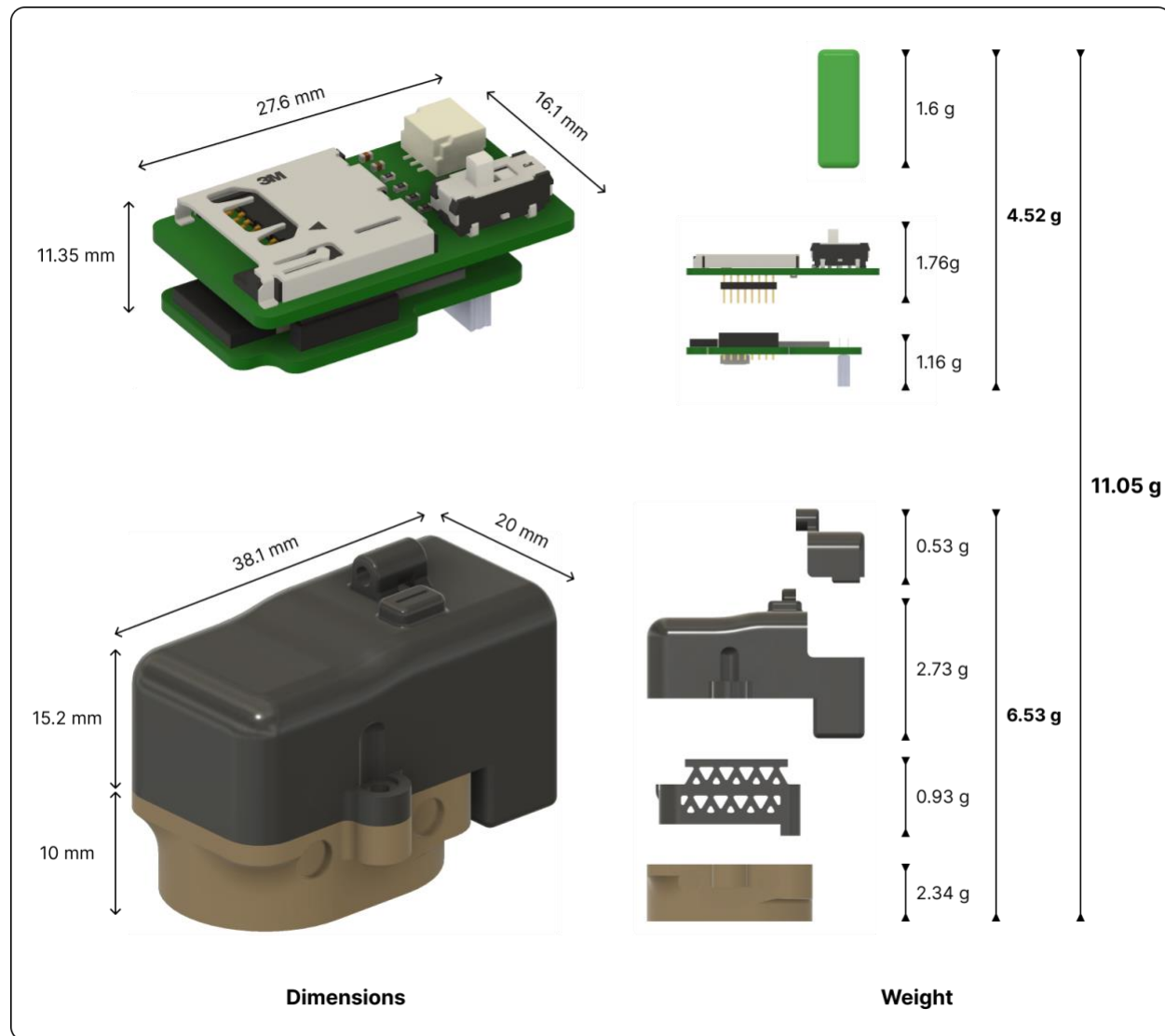


Figure 15: Assembly final dimensions and weight

Housing Toughness

Finite element analysis (FEA) simulations were performed on the top housing to assess the design's toughness. The first (Figure 16) applies a 110 N load on the housing's top surfaces to simulate the fall of a 350g marmoset from 0.5 meters, assuming an impact duration of 0.01 seconds. The resulting safety factor is 2.151, meaning the design can handle 2.151x the stress before failure.

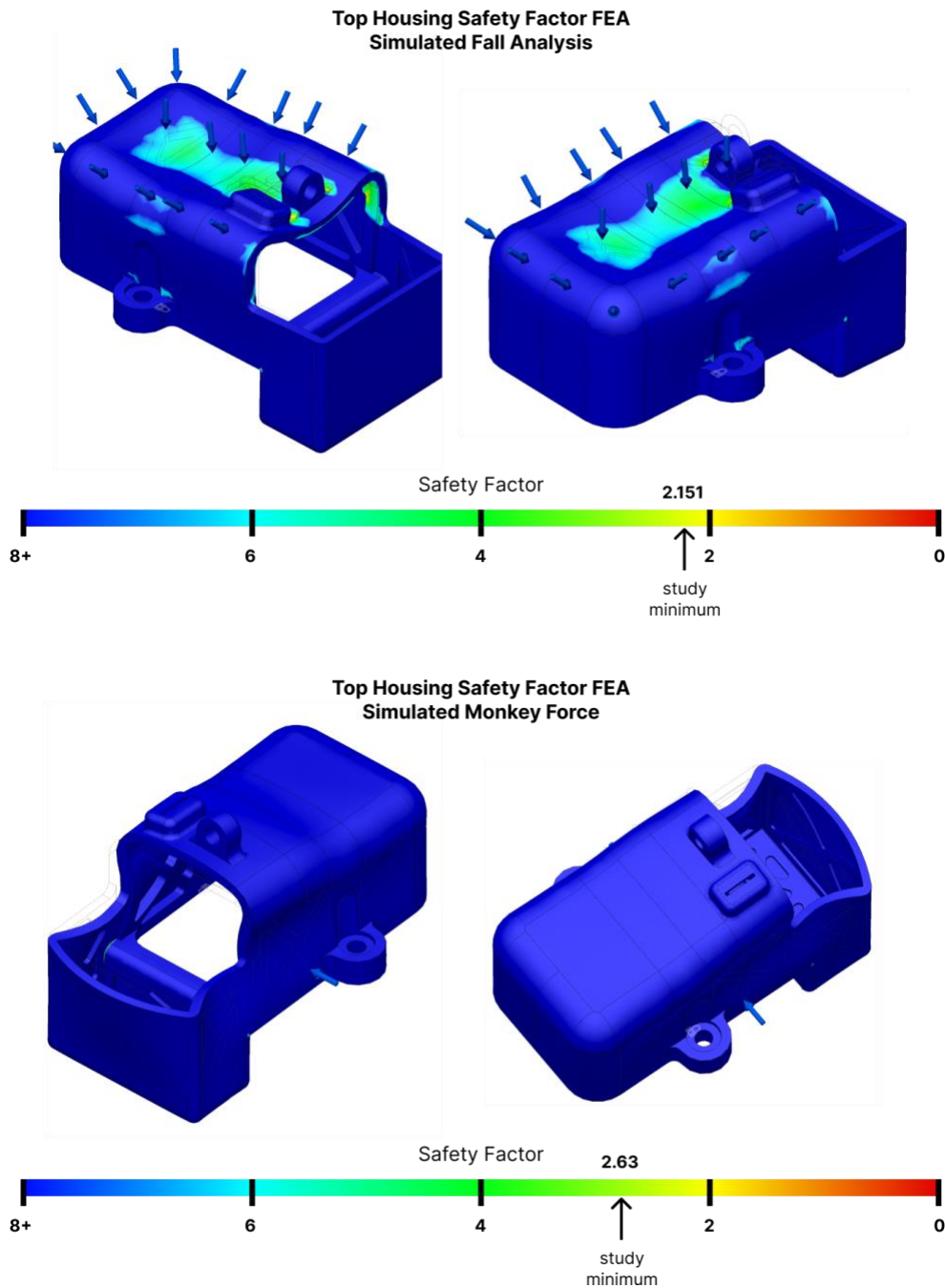


Figure 16: FEA simulations (deformations exaggerated for illustration)

A lateral force study assessed the design's robustness to monkey inquisitiveness, assuming the marmosets can exert forces up to five times their body weight. This yields 1.75 kgf (kilogram-force) or ~17 N. The study yields a minimum safety factor of 2.63.

Assembly & Disassembly Time

Lastly, the assembly, disassembly, and battery swap times were measured (Appendix: Figure 24). An electric screwdriver was used in the process. Assembling the device takes 1.5 minutes, the disassembly takes 1 minute, and, importantly, battery swaps are a 30-second process.

6. Discussion

The prototype's development and testing have yielded promising results, demonstrating its potential as a lightweight, efficient marmoset neural logger. Despite testing on a breadboard prototype, the system's performance exceeded many initial specifications (Table 7).

The logger successfully acquired and processed neural data, producing clean, interpretable signals, as evidenced by the 10 Hz sinusoidal test signal. The system demonstrated stable performance up to 750 Hz sampling rate per channel, covering the full LFP range. While this falls short of capturing action potentials, it significantly exceeds the initial 100 Hz/channel specification for a device of this size and power consumption.

Power management and autonomy were critical considerations. The prototype exhibited an estimated autonomy of 2 hours and 40 minutes using an 80 mAh battery at a 500 Hz sampling rate. These results are great considering the simultaneous local storage and wireless transmission capabilities. The power consumption breakdown revealed SD card operations as the primary power draw, suggesting that BLE-only operations could significantly extend autonomy (~5 hrs at 500 Hz) at the cost of reduced data throughput. Notably, a larger 300 mAh battery could quadruple the autonomy to around 20 hours in BLE-only mode, adding only ~6g.

The mechanical design represents a significant advancement in miniaturisation for marmoset neural recording devices. The final assembly, including the crown and battery, weighs just 11.05 grams and measures 25.2 x 38.1 x 20 mm, approximately 3% of a typical marmoset's body weight. This surpasses many existing solutions in the literature. Despite its lightweight design, FEA simulations suggest the housing is robust enough to withstand accidental falls and the monkey's manipulation, with safety factors exceeding 2. Lastly, the operation times are all under the 2-minute mark, demonstrating an elevated ease-of-use and minimal disturbances to marmoset welfare.

Table 4: Specification achievement levels

Spec	Minimum Target	Completion
E1 - Autonomy	2 hrs	Surpassed
E2 - Channel Count	≥16	Achieved
E3 - Sampling Rate	100 Hz/channel	Surpassed
M1 - Dimensions	40 x 70 x 40	Surpassed
M2 - Weight	12 g	Surpassed
M3 - Durability	High	Achieved
P1 - Wireless Range	≥ 5m	Not tested (prototype not matching final PCB antenna)
P2 - Latency	< 10 ms	Surpassed
P3 - Local Storage & Wireless	Yes	Achieved
D1 - Plug & Play	Under 2 min	Surpassed
D2 - Remote Operation	Yes	Not Achieved

When compared to existing solutions, the logger demonstrates several advantages. It is roughly half the weight and volume of the best research marmoset logger (12). While some commercial systems like FreeLynx (54) offer higher sampling rates, this device outperforms in size and weight, being smaller and about half as heavy. Our sampling rate per channel surpasses that of ONEIROS (23), another system capable of wireless transmission and SD card storage. However, ONEIROS cannot perform these functions simultaneously as our device can.

However, this system has limitations. While suitable for LFPs, the current sampling rate is insufficient for APs. The total failure in BLE-only mode at 1500 Hz also points to a mismanaged RHD2132 sampling, as the system should be less constrained without parallel SD card logging. The missing PCB also prevented the BLE range from being tested. Lastly, the initially planned remote operation functionality is not yet implemented.

Looking ahead, several avenues for improvement and further development have been identified. Primarily, optimising the firmware presents the most immediate opportunity for enhancing performance. Implementing Direct Memory Access for the Intan RHD2132 interfacing could significantly increase speed and reduce CPU load. Refining thread scheduling and SD card usage patterns could also improve the maximum stable sampling frequency. Thread scheduling could benefit from leveraging work queues for lower-priority tasks such as the SD card and BLE.

Although initiated, developing a GUI for remote control and real-time data plotting remains to be completed. Channel activation, remapping, and RHD2132 configurations could be performed through the GUI to optimise ADC filters and amplifiers for lowered power consumption.

The PCB design could be improved by further leveraging both faces of the boards, potentially with a higher layer count. Additionally, lower-profile components could reduce the height of the PCB-stack, and external adapters could remove the need for specialised connectors for firmware flashing. A low-hanging fruit component to replace would be the mechanical switch with a lower-profile magnetic switch, potentially increasing the ease-of-use.

Device dimensions could be reduced on the mechanical front through alternative PCB boards without SD logging, enabling BLE-only operation in a smaller package. Additionally, further mechanical design versions could be developed to “shrink wrap” the PCB in housing and optimise all gaps. Whilst unsuccessful iterations were conducted with generative design to sustain the target loads and computationally reduce housing weight, further work in this avenue could yield improvements.

7. Conclusion

This project has developed a novel, lightweight neural logger for marmoset monkeys, combining miniaturisation, wireless capabilities, and local storage in a package that significantly reduces animal impact. Key achievements include a miniaturised, robust package weighing 11.05 g, stable performance up to 750 Hz sampling rate per channel (12,000 S/s total), and simultaneous local storage and wireless transmission with sub-10 ms latencies. The device's potential impact on neuroscience research is significant, enabling more naturalistic behavioural studies and offering novel flexibility in experimental design and data collection. While areas for improvement remain (e.g., increasing sampling rate for action potential capture, implementing remote operation), this project lays a foundation for future developments. Such tools represent vital steps in neurotechnology research towards less invasive loggers, maximising animal welfare and ultimately contributing to human healthcare applications.

Acknowledgements

I want to express my gratitude to Professor Tim Constandinou for trusting and supporting me in this ambitious project, with expectations reaching beyond the usual context of a Masters Project and extending into a collaborative study with the University of Newcastle. I am also extremely grateful for Dr. Ian Williams' continuous support throughout the development process, from teaching me tools to tediously helping me get testing equipment up and running. This report and my results would not be of this quality without your help. I would also like to thank Dr. Yuki Kikuchi and the entire team at Newcastle University for being so welcoming and allowing me to ask questions non-stop during the marmoset surgery I was lucky to attend. Thank you to my friends -you know who you are- for always being there when work gets difficult. And lastly, thank you to my parents for their unwavering support through yet another step of my academic journey.

References

1. Ngo HV V., Martinetz T, Born J, Mölle M. Auditory closed-loop stimulation of the sleep slow oscillation enhances memory. *Neuron*. 2013;78(3): 545–553. <https://doi.org/10.1016/j.neuron.2013.03.006>.
2. Moreira CG, Baumann CR, Scandella M, Nemirovsky SI, Leach S, Huber R, et al. Closed-loop auditory stimulation method to modulate sleep slow waves and motor learning performance in rats. *eLife*. 2021;10. <https://doi.org/10.7554/ELIFE.68043>.
3. Jourde HR, Merlo R, Brooks M, Rowe M, Coffey EBJ. The neurophysiology of closed-loop auditory stimulation in sleep: A magnetoencephalography study. *European Journal of Neuroscience*. 2024;59(4): 613–640. <https://doi.org/10.1111/EJN.16132>.
4. Garcia-Molina G, Tsoneva T, Neff A, Salazar J, Bresch E, Grossekathofer U, et al. Hybrid in-phase and continuous auditory stimulation significantly enhances slow wave activity during sleep. *Proceedings of the Annual International Conference of the IEEE Engineering in Medicine and Biology Society, EMBS*. 2019; 4052–4055. <https://doi.org/10.1109/EMBC.2019.8857678>.
5. Karalis N, Dejean C, Chaudun F, Khoder S, R Rozeske R, Wurtz H, et al. 4-Hz oscillations synchronize prefrontal–amygdala circuits during fear behavior. *Nature Neuroscience* 2016 19:4. 2016;19(4): 605–612. <https://doi.org/10.1038/nn.4251>.
6. Chen S, Tan Z, Xia W, Gomes CA, Zhang X, Zhou W, et al. Theta oscillations synchronize human medial prefrontal cortex and amygdala during fear learning. *Science Advances*. 2021;7(34): 4198–4216. https://doi.org/10.1126/SCIADV.ABF4198/SUPPL_FILE/SCIADV.ABF4198_SM.PDF.
7. Taub AH, Perets R, Kahana E, Paz R. Oscillations Synchronize Amygdala-to-Prefrontal Primate Circuits during Aversive Learning. *Neuron*. 2018;97(2): 291–298.e3. <https://doi.org/10.1016/J.NEURON.2017.11.042/ASSET/579F54DA-A13D-4C0C-8658-A59ADD2B8255/MAIN.ASSETS/GR4.JPG>.
8. Vytal KE, Overstreet C, Charney DR, Robinson OJ, Grillon C. Sustained anxiety increases amygdala–dorsomedial prefrontal coupling: a mechanism for maintaining an anxious state in healthy adults. *Journal of Psychiatry & Neuroscience : JPN*. 2014;39(5): 321. <https://doi.org/10.1503/JPN.130145>.
9. Drevets WC. Neuroimaging Abnormalities in the Amygdala in Mood Disorders. *Annals of the New York Academy of Sciences*. 2003;985(1): 420–444. <https://doi.org/10.1111/J.1749-6632.2003.TB07098.X>.
10. LeDoux J. The emotional brain, fear, and the amygdala. *Cellular and Molecular Neurobiology*. 2003;23(4–5): 727–738. <https://doi.org/10.1023/A:1025048802629/METRICS>.
11. LeDoux J. The amygdala. *Current Biology*. 2007;17(20): R868–R874. <https://doi.org/10.1016/j.cub.2007.08.005>.
12. Walker JD, Pirsche F, Sundiang M, Niekrasz M, MacLean JN, Hatsopoulos NG. Chronic wireless neural population recordings with common marmosets. *Cell Reports*. 2021;36(2): 109379. <https://doi.org/10.1016/j.celrep.2021.109379>.

13. Prins NW, Pohlmeier EA, Debnath S, Mylavarapu R, Geng S, Sanchez JC, et al. Common marmoset (*Callithrix jacchus*) as a primate model for behavioral neuroscience studies. *Journal of Neuroscience Methods*. 2017;284: 35–46. <https://doi.org/10.1016/J.JNEUMETH.2017.04.004>.
14. Okano H, Hikishima K, Iriki A, Sasaki E. The common marmoset as a novel animal model system for biomedical and neuroscience research applications. *Seminars in Fetal and Neonatal Medicine*. 2012;17(6): 336–340. <https://doi.org/10.1016/J.SINY.2012.07.002>.
15. Miller CT, Freiwald WA, Leopold DA, Mitchell JF, Silva AC, Wang X. Marmosets: A Neuroscientific Model of Human Social Behavior. *Neuron*. 2016;90(2): 219–233. [https://doi.org/10.1016/J.NEURON.2016.03.018/ASSET/ICED1E09-C316-42B7-8019-8C1F8F8CC582/MAIN.ASSETS/GRI.JPG](https://doi.org/10.1016/J.NEURON.2016.03.018).
16. Zhao L, Wang X. Frontal cortex activity during the production of diverse social communication calls in marmoset monkeys. *Nature Communications* 2023 14:1. 2023;14(1): 1–17. <https://doi.org/10.1038/s41467-023-42052-5>.
17. Cavanagh JF. Electrophysiology as a theoretical and methodological hub for the neural sciences. *Psychophysiology*. 2019;56(2): e13314. <https://doi.org/10.1111/PSYP.13314>.
18. Takahashi S; A, Panuccio G, Patrick E, Ide K, Takahashi S. A Review of Neurologgers for Extracellular Recording of Neuronal Activity in the Brain of Freely Behaving Wild Animals. *Micromachines* 2022, Vol. 13, Page 1529. 2022;13(9): 1529. <https://doi.org/10.3390/MI13091529>.
19. Gilja V, Chestek CA, Nuyujukian P, Foster J, Shenoy K V. Autonomous head-mounted electrophysiology systems for freely behaving primates. *Current Opinion in Neurobiology*. 2010;20(5): 676–686. <https://doi.org/10.1016/J.CONB.2010.06.007>.
20. Cheng N, Murari K. OSERR: an open-source standalone electrophysiology recording system for rodents. *Scientific Reports*. 2020;10(1). <https://doi.org/10.1038/S41598-020-73797-4>.
21. Hsieh B. *Sleep studies in mice-open and closed loop devices for untethered recording and stimulation*. 2022.
22. Jiang Z, Huxter JR, Bowyer SA, Blockeel AJ, Butler J, Imtiaz SA, et al. TaiNi: Maximizing research output whilst improving animals' welfare in neurophysiology experiments. *Scientific Reports* 2017 7:1. 2017;7(1): 1–12. <https://doi.org/10.1038/s41598-017-08078-8>.
23. Massot B, Arthaud S, Barrillot B, Roux J, Ungurean G, Luppi PH, et al. ONEIROS, a new miniature standalone device for recording sleep electrophysiology, physiology, temperatures and behavior in the lab and field. *Journal of Neuroscience Methods*. 2019;316: 103–116. <https://doi.org/10.1016/J.JNEUMETH.2018.08.030>.
24. Ferrucci L, Nougaret S, Ceccarelli F, Sacchetti S, Fascianelli V, Benozzo D, et al. Social monitoring of actions in the macaque frontopolar cortex. *Progress in Neurobiology*. 2022;218: 102339. <https://doi.org/10.1016/J.PNEUROBIO.2022.102339>.
25. Fernandez-Leon JA, Parajuli A, Franklin R, Sorenson M, Felleman DJ, Hansen BJ, et al. A wireless transmission neural interface system for unconstrained non-human primates. *Journal of Neural Engineering*. 2015;12(5): 056005. <https://doi.org/10.1088/1741-2560/12/5/056005>.
26. Vyssotski AL, Serkov AN, Itskov PM, Dell'Omo G, Latanov A V., Wolfer DP, et al. Miniature neurologgers for flying pigeons: Multichannel EEG and action and field potentials in combination with GPS recording. *Journal of Neurophysiology*. 2006;95(2): 1263–1273. <https://doi.org/10.1152/JN.00879.2005/ASSET/IMAGES/LARGE/Z9K0020672040009.JPG>.
27. *RHD Recording System / Intan Technologies*. https://intantech.com/RHD_system.html [Accessed 1st March 2024].
28. *Connectors / Plexon*. <https://plexon.com/products/connectors/> [Accessed 30th August 2024].
29. *X-Headstage - Electrical Stimulation & Recording Headstage / NeuroNexus*. <https://www.neuronexus.com/products/x-headstage/> [Accessed 30th August 2024].
30. *Headstages / Cambridge NeuroTech*. <https://www.cambridgeneurotech.com/headstages> [Accessed 30th August 2024].

31. Headstage Pre-amplifiers – NeuralLynx. <https://neurallnx.fh-co.com/research-hardware/animal-interfaces/headstage-pre-amplifiers/#omnetics-headstages> [Accessed 30th August 2024].
32. Dhawale AK, Poddar R, Wolff SBE, Normand VA, Kopelowitz E, Ölveczky BP. Automated long-Term recording and analysis of neural activity in behaving animals. *eLife*. 2017;6. <https://doi.org/10.7554/ELIFE.27702>.
33. Harrison RR, Fotowat H, Chan R, Kier RJ, Olberg R, Leonardo A, et al. Wireless neural/EMG telemetry systems for small freely moving animals. *IEEE Transactions on Biomedical Circuits and Systems*. 2011;5(2): 103–111. <https://doi.org/10.1109/TBCAS.2011.2131140>.
34. Eliades SJ, Wang X. Chronic multi-electrode neural recording in free-roaming monkeys. *Journal of Neuroscience Methods*. 2008;172(2): 201–214. <https://doi.org/10.1016/J.JNEUMETH.2008.04.029>.
35. Ball D, Kliese R, Windels F, Nolan C, Stratton P, Sah P, et al. Rodent Scope: A User-Configurable Digital Wireless Telemetry System for Freely Behaving Animals. *PLOS ONE*. 2014;9(2): e89949. <https://doi.org/10.1371/JOURNAL.PONE.0089949>.
36. Roy S, Wang X. Wireless multi-channel single unit recording in freely moving and vocalizing primates. *Journal of Neuroscience Methods*. 2012;203(1): 28–40. <https://doi.org/10.1016/J.JNEUMETH.2011.09.004>.
37. Kim C, Jang A, Kim S, Cho S, Lee D, Kim YJ. A Wearable ECG Monitoring System Using Microneedle Electrodes for Small Animals. *IEEE Sensors Journal*. 2023;23(18): 21873–21881. <https://doi.org/10.1109/JSEN.2023.3300992>.
38. Chestek CA, Gilja V, Nuyujukian P, Kier RJ, Solzbacher F, Ryu SI, et al. HermesC: Low-power wireless neural recording system for freely moving primates. *IEEE Transactions on Neural Systems and Rehabilitation Engineering*. 2009;17(4): 330–338. <https://doi.org/10.1109/TNSRE.2009.2023293>.
39. Wang H, Ma Q, Chen K, Zhang H, Yang Y, Zheng N, et al. An Ultra-Low-Noise, Low Power and Miniaturized Dual-Channel Wireless Neural Recording Microsystem. *Biosensors* 2022, Vol. 12, Page 613. 2022;12(8): 613. <https://doi.org/10.3390/BIOS12080613>.
40. CerePlex W, Headstages / Products / Blackrock Neurotech. <https://blackrockneurotech.com/products/cereplex-w/> [Accessed 31st August 2024].
41. Yin M, Borton DA, Komar J, Agha N, Lu Y, Li H, et al. Wireless neurosensor for full-spectrum electrophysiology recordings during free behavior. *Neuron*. 2014;84(6): 1170–1182. <https://doi.org/10.1016/J.NEURON.2014.11.010/ATTACHMENT/EA66686F-9763-4D02-8CC4-EDED6EF15D96/MMC3.PDF>.
42. Gaidica M, Dantzer B. An implantable neurophysiology platform: Broadening research capabilities in free-living and non-traditional animals. *Frontiers in Neural Circuits*. 2022;16: 940989. <https://doi.org/10.3389/FNCIR.2022.940989/BIBTEX>.
43. Erofeev A, Antifeev I, Vinokurov E, Bezprozvanny I, Vlasova O. An Open-Source Wireless Electrophysiology System for In Vivo Neuronal Activity Recording in the Rodent Brain: 2.0. *Sensors* 2023, Vol. 23, Page 9735. 2023;23(24): 9735. <https://doi.org/10.3390/S23249735>.
44. Bluetooth 5 - nordicsemi.com. <https://www.nordicsemi.com/Products/Wireless/Bluetooth-Low-Energy/Bluetooth-5> [Accessed 1st September 2024].
45. Wu JY, Tang KT. A band-tunable, multichannel amplifier for neural recording with AP/LFP separation and dual-threshold adaptive AP detector. *Proceedings of the Annual International Conference of the IEEE Engineering in Medicine and Biology Society, EMBS*. 2011; 1847–1850. <https://doi.org/10.1109/IEMBS.2011.6090525>.
46. Luan S, Williams I, Maslik M, Liu Y, De Carvalho F, Jackson A, et al. Compact standalone platform for neural recording with real-time spike sorting and data logging. *Journal of Neural Engineering*. 2018;15(4): 046014. <https://doi.org/10.1088/1741-2552/AABC23>.
47. Harrison RR, Kier RJ, Chestek CA, Gilja V, Nuyujukian P, Ryu S, et al. Wireless Neural Recording With Single Low-Power Integrated Circuit. *IEEE transactions on neural systems and rehabilitation engineering : a publication of the IEEE Engineering in Medicine and Biology Society*. 2009;17(4): 322. <https://doi.org/10.1109/TNSRE.2009.2023298>.

48. *RHD2000 Amplifier Chips / Intan Technologies*. https://intantech.com/products_RHD2000.html [Accessed 1st September 2024].
49. Borna A, Najafi K. A low power light weight wireless multichannel microsystem for reliable neural recording. *IEEE Journal of Solid-State Circuits*. 2014;49(2): 439–451. <https://doi.org/10.1109/JSSC.2013.2293773>.
50. Jendritza P, Klein FJ, Fries P. Multi-area recordings and optogenetics in the awake, behaving marmoset. *Nature Communications* 2023;14:1. 2023;14(1): 1–16. <https://doi.org/10.1038/s41467-023-36217-5>.
51. Meyer AF, Poort J, O'Keefe J, Sahani M, Linden JF. A Head-Mounted Camera System Integrates Detailed Behavioral Monitoring with Multichannel Electrophysiology in Freely Moving Mice. *Neuron*. 2018;100(1): 46–60.e7. <https://doi.org/10.1016/j.neuron.2018.09.020>.
52. Mendrela AE, Kim K, English D, McKenzie S, Seymour JP, Buzsaki G, et al. A High-Resolution Opto-Electrophysiology System with a Miniature Integrated Headstage. *IEEE Transactions on Biomedical Circuits and Systems*. 2018;12(5): 1065–1075. <https://doi.org/10.1109/TBCAS.2018.2852267>.
53. Miranda H, Gilja V, Chestek CA, Shenoy K V., Meng TH. HermesD: A high-rate long-range wireless transmission system for simultaneous multichannel neural recording applications. *IEEE Transactions on Biomedical Circuits and Systems*. 2010;4(3): 181–191. <https://doi.org/10.1109/TBCAS.2010.2044573>.
54. FreeLynx – NeuralLynx. <https://neuralynx.fh-co.com/research-hardware/data-acquisition/freelyn/> [Accessed 1st September 2024].
55. MouseLog16C - Deuteron Technologies. <https://deuterontech.com/mouselog16c/> [Accessed 1st September 2024].
56. Broell LM, Hanshans C, Kimmerle D, Broell LM, Hanshans C, Kimmerle D. IoT on an ESP32: Optimization Methods Regarding Battery Life and Write Speed to an SD-Card. *Edge Computing - Technology, Management and Integration*. 2023; <https://doi.org/10.5772/INTECHOPEN.110752>.
57. Lui Gough. Experiment: microSD Card Power Consumption & SPI Performance. <https://goughlui.com/2021/02/27/experiment-microsd-card-power-consumption-spi-performance/>. <https://goughlui.com/2021/02/27/experiment-microsd-card-power-consumption-spi-performance/> [Accessed 6th September 2024].
58. SR44W Seiko Instruments | Battery Products | DigiKey. <https://www.digikey.be/en/products/detail/seiko-instruments/SR44W/7428840> [Accessed 2nd September 2024].
59. LR41 Murata Electronics | Mouser United Kingdom. https://www.mouser.co.uk/ProductDetail/Murata-Electronics/LR41?qs=l7cgNqFNUljPv84RIDn%252BCQ%3D%3D&srsId=AfmBOoqLNybpwlJ_xle4lRe5VYyXELKwA7HeCNJYzTSqJe-qvlRwrfe1 [Accessed 2nd September 2024].
60. cr1225.
61. Sa R. ZA13 maratone PR48 Hearing Aid Battery Swiss Made. www.renata.com
62. Small Lithium-polymer Battery 3.7V Rechargeable LP301013 23mAh 0.085Wh - Lithium_Polymer_Battery.net. <https://www.lithium-polymer-battery.net/small-lithium-polymer-battery-3-7v-rechargeable-lp301013-23mah-0-085wh/> [Accessed 2nd September 2024].
63. Micro Li-ion Battery LPM1254 3.6V 65mAh. <https://www.lithium-polymer-battery.net/micro-li-ion-battery-lpm1254-3-6v-65mah/> [Accessed 2nd September 2024].
64. Nazir G, Rehman A, Lee JH, Kim CH, Gautam J, Heo K, et al. A Review of Rechargeable Zinc–Air Batteries: Recent Progress and Future Perspectives. *Nano-Micro Letters* 2024;16:1. 2024;16(1): 1–44. <https://doi.org/10.1007/S40820-024-01328-1>.
65. 宋辉, 徐献芝, 李芬, Hui S, Xian-Zhi X, Fen L. 锌电极放电过程及失效机制数值分析. *物理化学学报*. 2013;29(09): 1961–1974. <https://doi.org/10.3866/PKU.WHXB201306144>.
66. Chestek CA, Gilja V, Nuyujukian P, Kier RJ, Solzbacher F, Ryu SI, et al. HermesC: Low-power wireless neural recording system for freely moving primates. *IEEE Transactions on Neural Systems and Rehabilitation Engineering*. 2009;17(4): 330–338. <https://doi.org/10.1109/TNSRE.2009.2023293>.

67. Grand L, Ftomov S, Timofeev I. Long-term synchronized electrophysiological and behavioral wireless monitoring of freely moving animals. *Journal of Neuroscience Methods*. 2013;212(2): 237–241. <https://doi.org/10.1016/J.JNEUMETH.2012.10.008>.
68. Home - Omnetics Connector Corp. <https://www.omnetics.com/> [Accessed 3rd September 2024].
69. Robinson NB, Krieger K, Khan F, Huffman W, Chang M, Naik A, et al. The current state of animal models in research: A review. *International Journal of Surgery*. 2019;72: 9–13. <https://doi.org/10.1016/J.IJSU.2019.10.015>.
70. Angius D, Wang H, Spinner RJ, Gutierrez-Cotto Y, Yaszemski MJ, Windebank AJ. A systematic review of animal models used to study nerve regeneration in tissue-engineered scaffolds. *Biomaterials*. 2012;33(32): 8034–8039. <https://doi.org/10.1016/J.BIOMATERIALS.2012.07.056>.
71. Etholm L, Arabadzisz D, Lipp HP, Heggelund P. Seizure logging: A new approach to synchronized cable-free EEG and video recordings of seizure activity in mice. *Journal of Neuroscience Methods*. 2010;192(2): 254–260. <https://doi.org/10.1016/J.JNEUMETH.2010.08.003>.
72. Sattler NJ, Wehr M. A Head-Mounted Multi-Camera System for Electrophysiology and Behavior in Freely-Moving Mice. *Frontiers in Neuroscience*. 2021;14: 592417. [https://doi.org/10.3389/FNINS.2020.592417/BIBTEX](https://doi.org/10.3389/FNINS.2020.592417).
73. Sun NL, Lei YL, Kim BH, Ryou JW, Ma YY, Wilson FAW. Neurophysiological recordings in freely moving monkeys. *Methods*. 2006;38(3): 202–209. <https://doi.org/10.1016/J.YMETH.2005.09.018>.
74. Buzsáki G, Stark E, Berényi A, Khodagholy D, Kipke DR, Yoon E, et al. Tools for probing local circuits: High-density silicon probes combined with optogenetics. *Neuron*. 2015;86(1): 92–105. [https://doi.org/10.1016/J.NEURON.2015.01.028/ASSET/62E2FE19-079C-4BA1-BE86-060726AC6A1B/MAIN.ASSETS/GR4.JPG](https://doi.org/10.1016/J.NEURON.2015.01.028).
75. Schwarz DA, Lebedev MA, Hanson TL, Dimitrov DF, Lehew G, Meloy J, et al. Chronic, wireless recordings of large-scale brain activity in freely moving rhesus monkeys. *Nature Methods* 2014 11:6. 2014;11(6): 670–676. <https://doi.org/10.1038/nmeth.2936>.
76. Fraser D, Weary DM, Pajor EA, Milligan BN. A Scientific Conception of Animal Welfare that Reflects Ethical Concerns. *Animal Welfare*. 1997;6(3): 187–205. <https://doi.org/10.1017/S0962728600019795>.
77. King M, Zohny H. Animal researchers shoulder a psychological burden that animal ethics committees ought to address. *J Med Ethics*. 2021;0: 1–5. <https://doi.org/10.1136/medethics-2020-106945>.
78. VisiJet ® M2S-HT90 Production Rigid.
79. ISP1807. <https://www.insightsip.com/products/bluetooth-smart-modules/isp1807> [Accessed 7th September 2024].
80. BT840F, BT840, BT840E, BT840N, BT840NE nRF52840 5.3, 802.15.4 Modules, with nRF21540.
81. A guide to speed classes for SD and microSD Cards - Kingston Technology. <https://www.kingston.com/unitedkingdom/en/blog/personal-storage/memory-card-speed-classes> [Accessed 6th September 2024].
82. Part Numbering Information MT FC-Micron Technology Product Family FC = NAND Flash + controller NAND Density NAND Component Controller ID Production Status Blank = Production ES = Engineering sample. 2015; www.micron.com/decoder.
83. MT29F128G08AJAAAWP-ITZ: A Micron | Mouser United Kingdom. <https://www.mouser.co.uk/ProductDetail/Micron/MT29F128G08AJAAAWP-ITZA?qs=rrS6Pyft74djZxgbI%2F0r5Q%3D%3D> [Accessed 6th September 2024].
84. ADS1298 data sheet, product information and support | TI.com. <https://www.ti.com/product/ADS1298> [Accessed 7th September 2024].
85. ADS1299 data sheet, product information and support | TI.com. <https://www.ti.com/product/ADS1299#features> [Accessed 7th September 2024].

Appendix

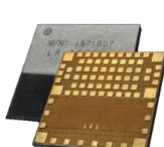
Newcastle University Ethical Statement

As per Appendix G of the Home Office Guidance on the Operation of the Animals (Scientific Procedures) Act 1986, regarding severity classification, such research needs to be prospectively classified as severe. This recognises the sensitive nature of research with nonhuman primates and the possibility, however, remote of any animal suffering severely. To minimise this risk, the Home Office approved PPL (PPL PP8119034: Kikuchi as Project License Holder), which this marmoset study will be under, is structured such that the humane endpoints are in place to prevent any animal suffering severely and to reduce cumulative impact to a bare minimum, by for example providing sufficient spacing between moderate severity events.

Extra MCU Selection Considerations

Additional MCU options considered included the nRF5340 and STM32 series. The nRF5340's dual-core architecture was deemed unnecessary for current requirements. The STM32 series, while powerful, lacked the ease of firmware development and BLE compatibility in their low-power line. It was also less prevalent in the literature review. The nRF52840's LLPM package in the nRF Connect SDK, providing 1-ms latencies using BLE, was a key advantage over the nRF5340. The selection process prioritised power efficiency, processing capability, wireless capabilities, memory, peripheral support, development environment, and integrated module availability.

Table 5: nRF52840 modules comparison

	ISP1807 (79)	BT840F (80)
Image (from reference)		
Dimensions (mm)	8 x 8 x 1	15 x 20.8 x 1.9
Operating Voltage (V)	1.7-3.6	1.7-5.5
TX Current @8dBm (mA)	16.4	13.6

Extra Storage Support Selection Considerations

Table 6: Storage support comparison

	SD Card (57,81)	eMMC (82)	NAND Chip (83)
Capacity (GB)	1 - 2000	2 - 512	1 - 1000
Form Factor	Removable Card	Chip	Chip
Interface	SPI	SDIO	Custom

Write Speed (MB/s)	~10	~45	~1000
Active Current (mA)	150	150	50
Idle Current (mA)	0.1	0.1	0.1
Wear Levelling	Built-In	Built-In	External Controller
Ease of Replacement	Very Easy	Difficult	Difficult
MCU Integration Complexity	Easy	Difficult	Difficult

Extra ADC Selection Considerations

The TI ADS1298 and ADS1299 offer 24-bit resolution compared to the Intan's 16-bit, but their 8-channel limitation and higher power consumption made them less suitable for this application. The custom op-amp solution, while offering more design flexibility, was not pursued due to increased development time and complexity without significant advantages over the integrated Intan solution. The RHD2132's ready availability was also a factor in its selection.

Table 7: Analog front-end options comparison

	RHD2116/RHD2132 (48)	ADS1298/ADS1299 (84,85)
Dimensions (mm)	8 x 8	8x8/12x12
Weight (g)	0.168	0.24
Max Sampling Rate (kS/s/channel)	30	32/16
Channel Count	16/32	8
ADC Bit Depth	16	24
Input Referred Noise (μVrms)	2.4	0.6/0.15
Current Draw (250 S/s) (mA)	1.01/1.08	5.3/8
MCU Integration Complexity	Medium	Medium

Firmware

Developing the firmware was a particularly long part of the system's development. It involved a continuous iterative process of incremental improvements to ensure the coexistence of many high-speed, time-critical operations. The firmware is built around the nRFConnect SDK, which itself relies on Zephyr RTOS. It totals 1900 lines of embedded C code and 2000 lines of Python data-unpacking and results plotting logic.

The firmware and Python code is available at: https://github.com/Lampadare/MARM_fmw_v0

System Development Extra Figures

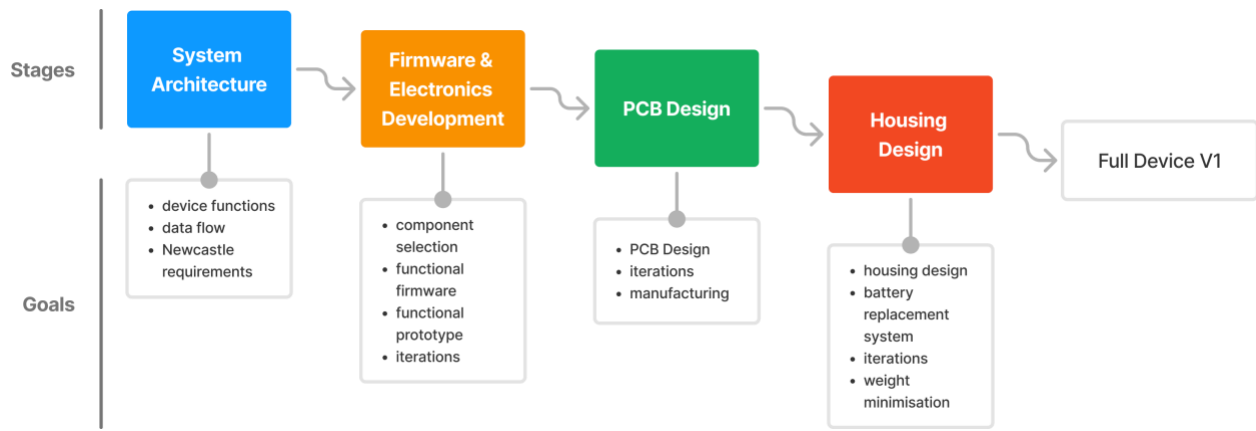


Figure 17: System development process

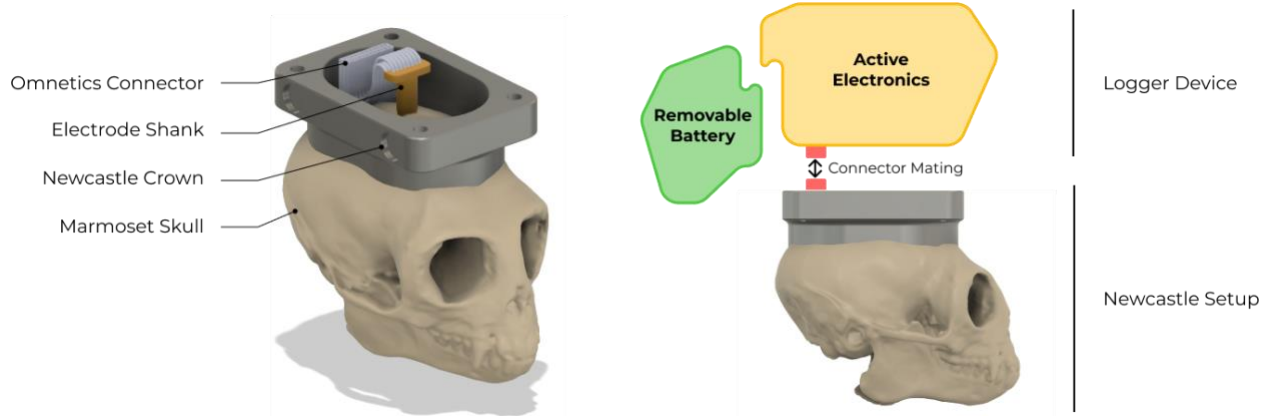


Figure 18: Marmoset skull with planned electrode and chamber setup (left), original device plan (right)

Firmware Extra Figures

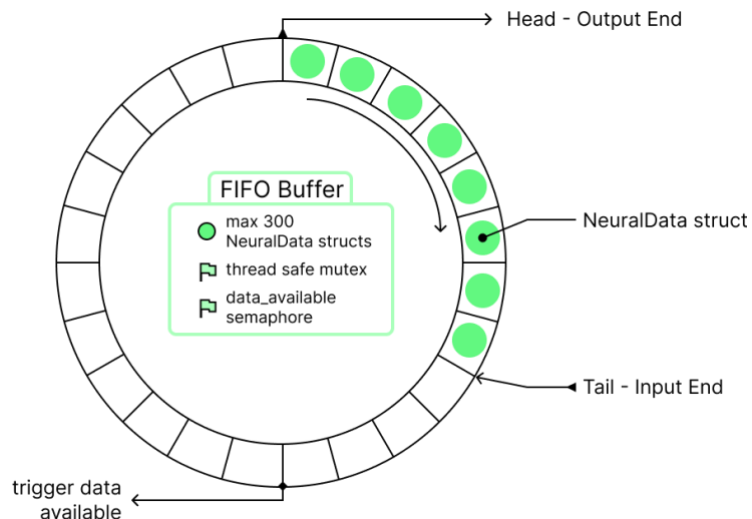


Figure 19: FIFO buffer diagram

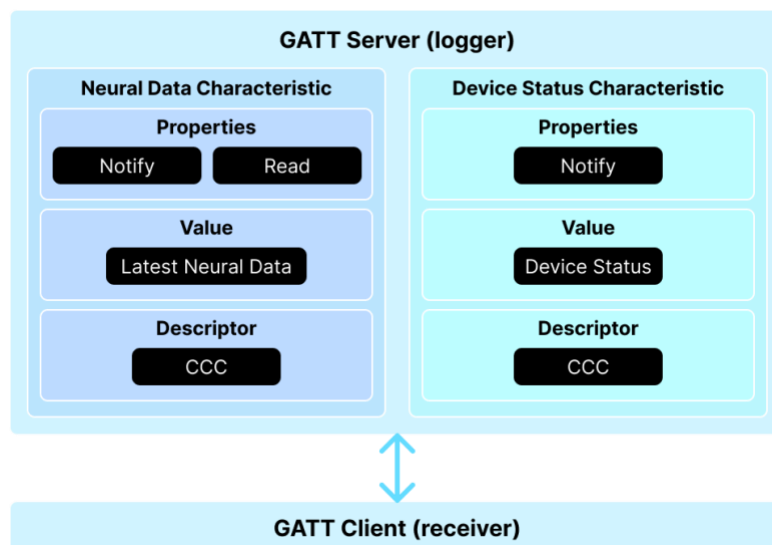


Figure 20: Neural Bluetooth Service GATT

PCB Design Extra Figures

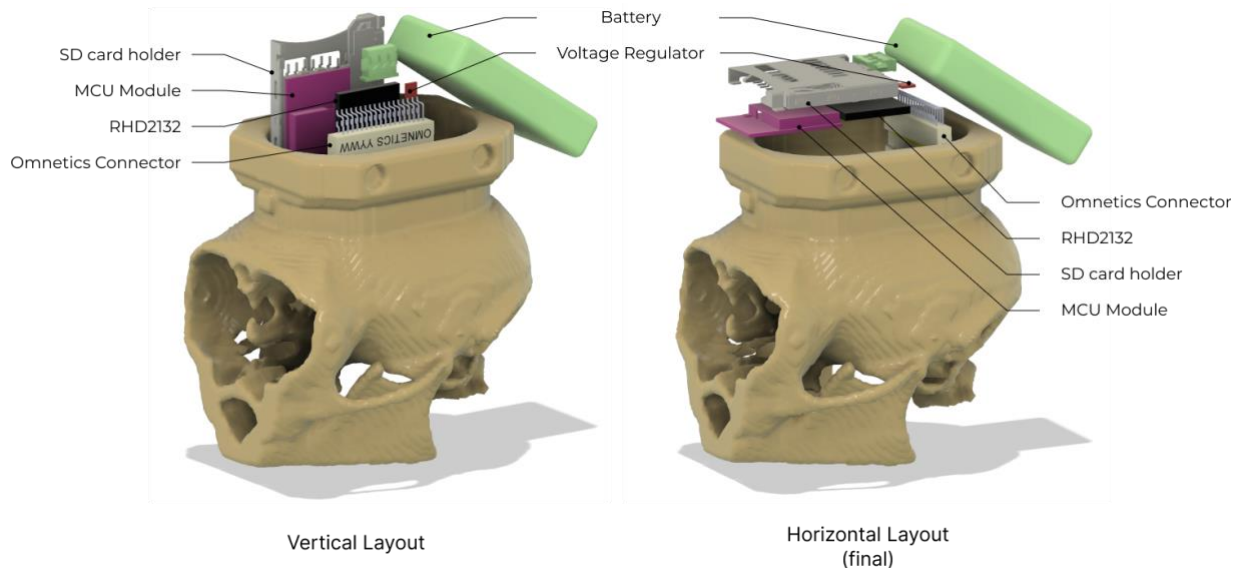


Figure 21: Initial component layout iterations

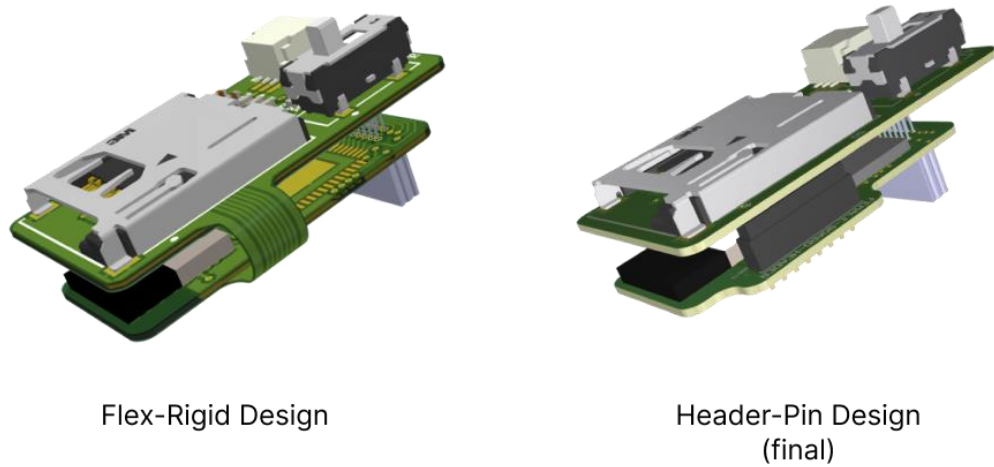


Figure 22: PCB design iterations

Mechanical Design Extra Figures



Figure 23: FDM prototypes printing process (left), finalised prototypes (right)

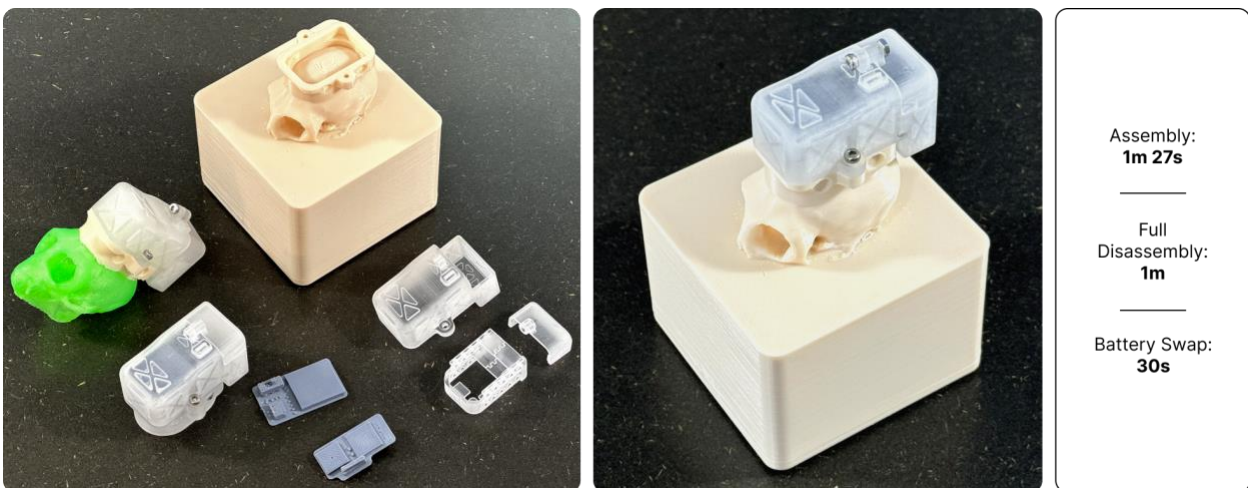


Figure 24: Final mechanical prototype and assembly times

Results Extra Figures

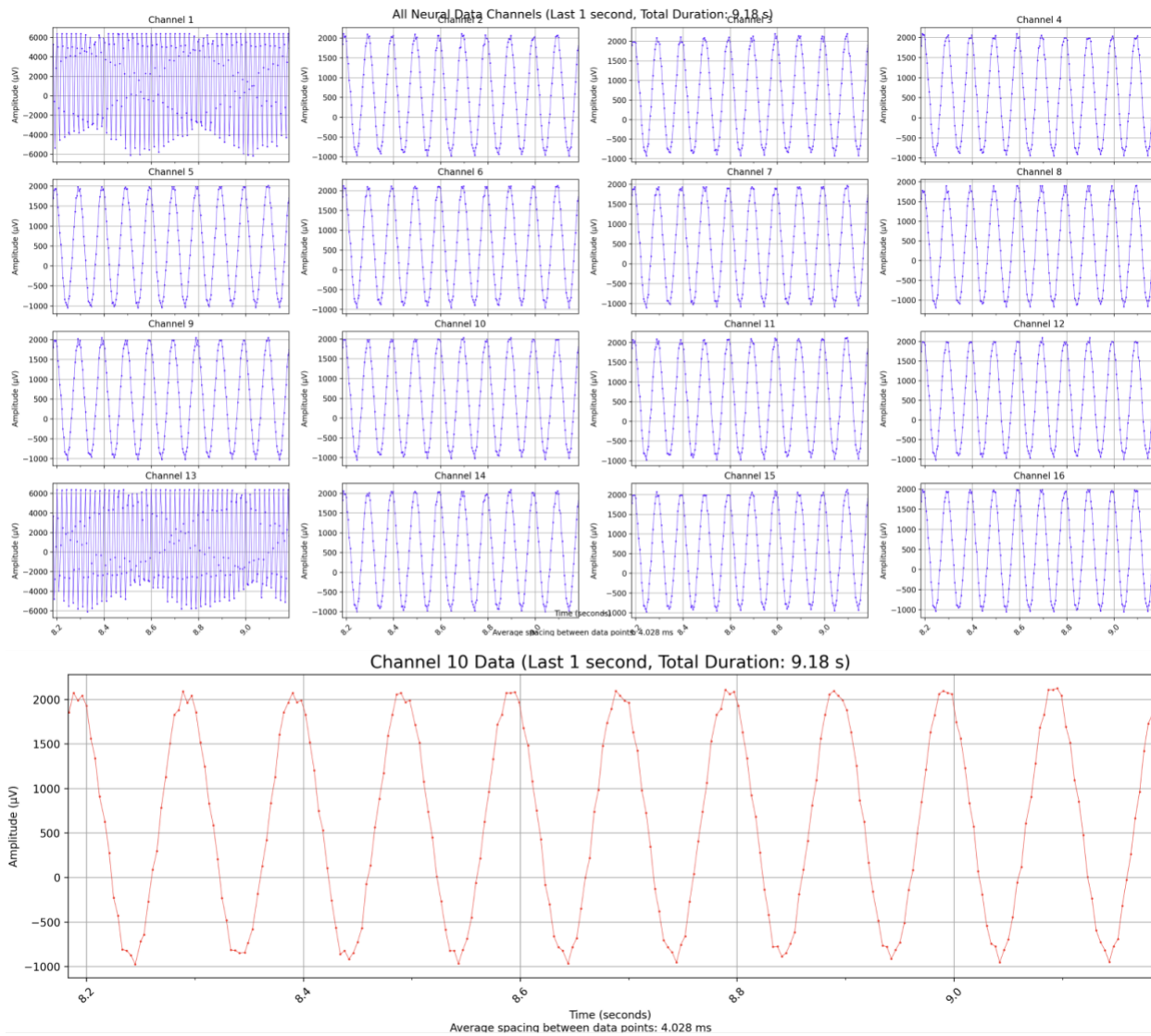


Figure 25: 10Hz sinusoidal signal recorded with logger sampling at 250 Hz (all channels connected together, channels 1 and 13 are different due to the prototype wiring)

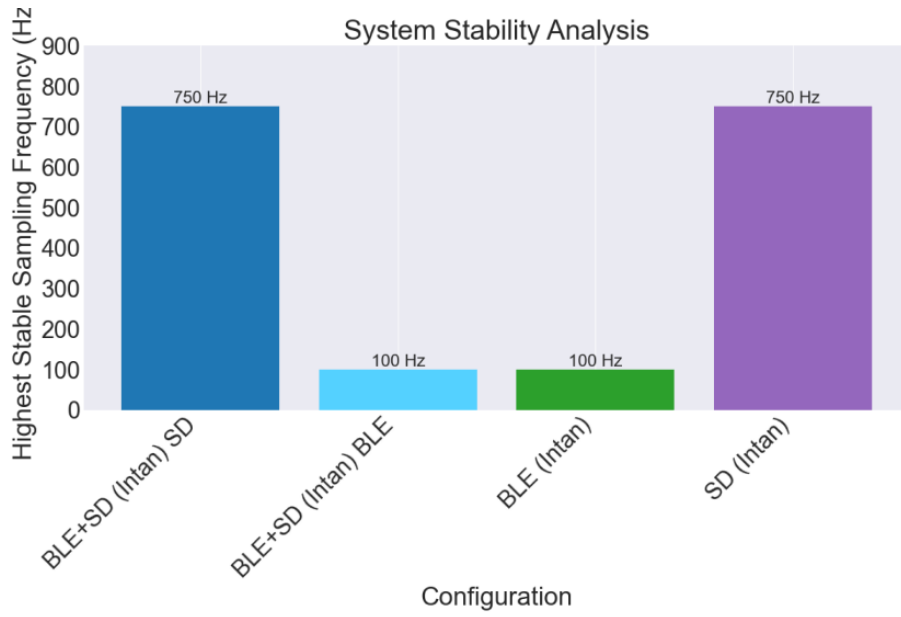


Figure 26: System stability (max 100 packets lost, 10 second recording window)

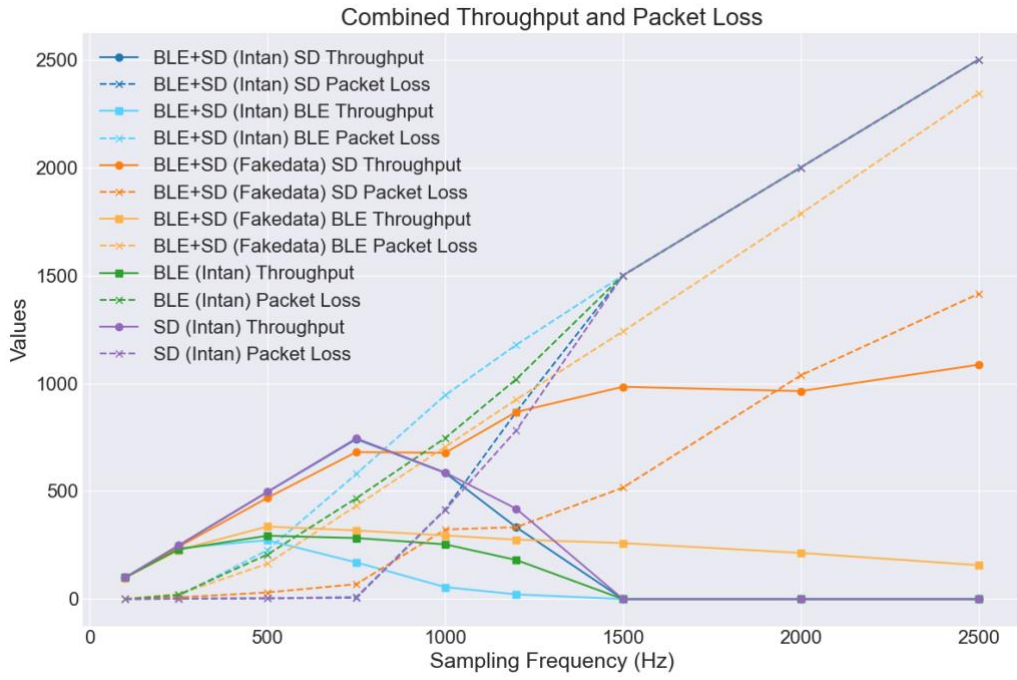


Figure 27: Combined throughput and packets lost analysis

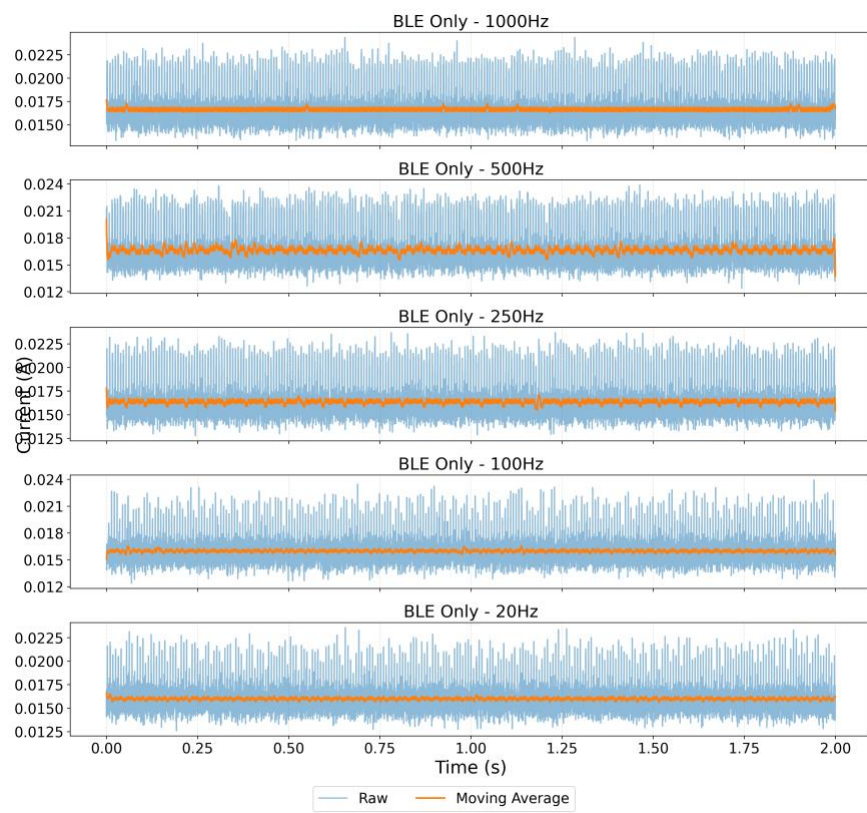


Figure 28: Power Consumption BLE only, RHD2132 sampling

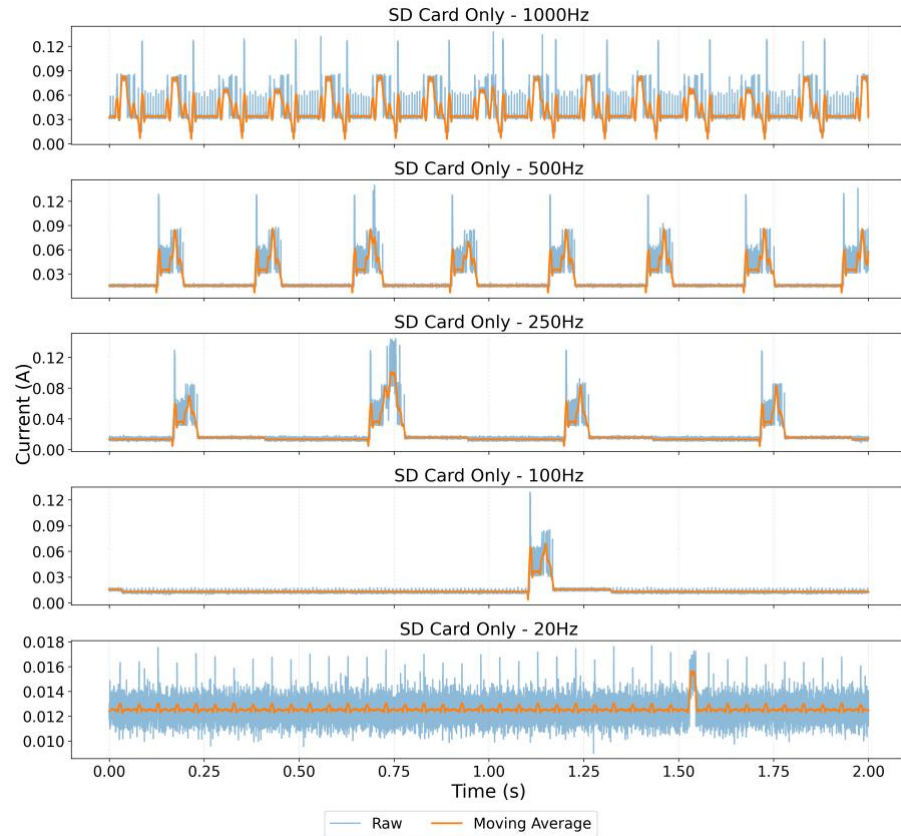


Figure 29: Power Consumption SD only, RHD2132 sampling

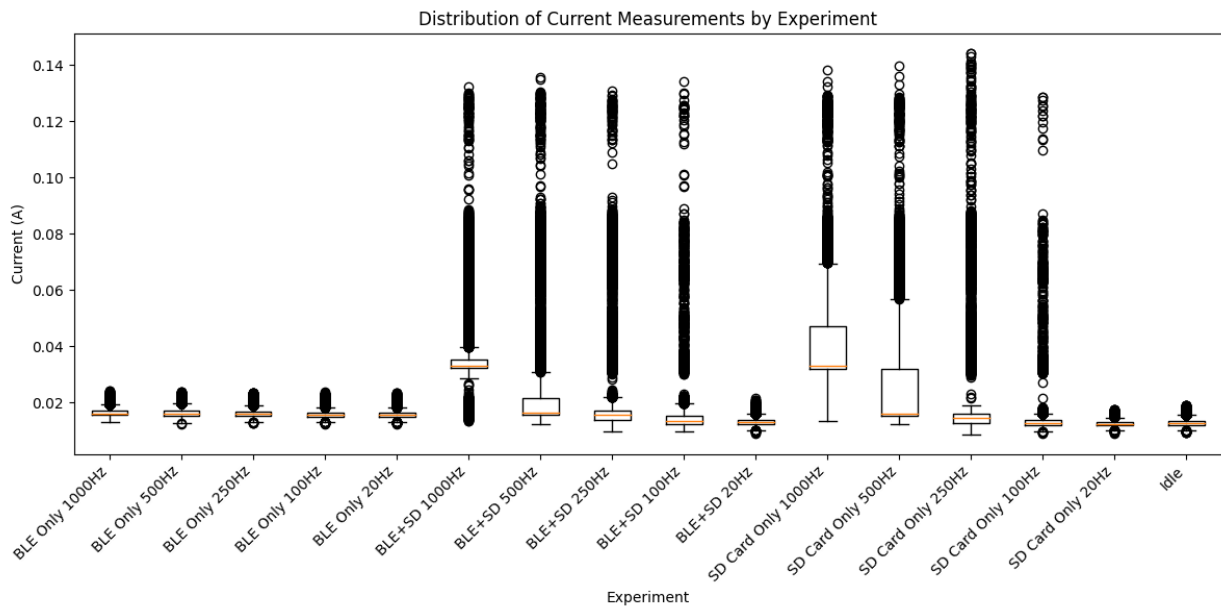


Figure 30: Current measurement boxplot by experiment